12-2014

Recruitment Facilitation and Spatial Pattern Formation in Soft-Bottom Mussel Beds

John A. Commito
Gettysburg College

Ann E. Commito
Frederick Community College

Rutherford V. Platt
Gettysburg College

Benjamin M. Grupe
Gettysburg College

Wendy Dow Piniak
Gettysburg College

Recommended Citation

John A. Commito, Ann E. Commito, Rutherford V. Platt, Benjamin M. Grupe, Wendy E. Dow Piniak, Natasha J. Gownaris, Kyle A. Reeves, and Allison M. Vissichelli. "Recruitment Facilitation and Spatial Pattern Formation in Soft-Bottom Mussel Beds." Ecosphere 5.12 (December 2014), Article 160.

Recruitment Facilitation and Spatial Pattern Formation in Soft-Bottom Mussel Beds

Abstract

Mussels (*Mytilus edulis*) build massive, spatially complex, biogenic structures that alter the biotic and abiotic environment and provide a variety of ecosystem services. Unlike rocky shores, where mussels can attach to the primary substrate, soft sediments are unsuitable for mussel attachment. We used a simple lattice model, field sampling, and field and laboratory experiments to examine facilitation of recruitment (i.e., preferential larval, juvenile, and adult attachment to mussel biogenic structure) and its role in the development of power-law spatial patterns observed in Maine, USA, soft-bottom mussel beds. The model demonstrated that recruitment facilitation produces power-law spatial structure similar to that in natural beds. Field results provided strong evidence for facilitation of recruitment to other mussels—they do not simply map onto a hard-substrate template of gravel and shell hash. Mussels were spatially decoupled from non-mussel hard substrates to which they can potentially recruit. Recent larval recruits were positively correlated with adult mussels, but not with other hard substrates. Mussels made byssal thread attachments to other mussels in much higher proportions than to other hard substrates. In a field experiment, mussel recruitment was highest to live mussels, followed by mussel shell hash and gravel, with almost no recruitment to muddy sand. In a laboratory experiment, evenly dispersed mussels rapidly self-organized into power-law clusters similar to those observed in nature. Collectively, the results indicate that facilitation of recruitment to existing mussels plays a major role in soft-bottom spatial pattern development. The interaction between large-scale resource availability (hard substrate) and local-scale recruitment facilitation may be responsible for creating complex power-law spatial structure in soft-bottom mussel beds.

Keywords

fractal power-law, Maine, mussel beds, Mytilus edulis, recruitment facilitation, self-organization, soft-bottom, spatial pattern

Disciplines

Animal Sciences | Aquaculture and Fisheries | Environmental Monitoring | Environmental Sciences

Authors

John A. Commito, Ann E. Commito, Rutherford V. Platt, Benjamin M. Grupe, Wendy Dow Piniak, Natasha J. Gownaris, Kyle A. Reeves, and Allison M. Vissichelli

esa

ECOSPHERE

Recruitment facilitation and spatial pattern formation in soft-bottom mussel beds

JOHN A. COMMITO,[1,2,]† ANN E. COMMITO,[3] RUTHERFORD V. PLATT,[1] BENJAMIN M. GRUPE,[1,4] WENDY E. DOW PINIAK,[1,5] NATASHA J. GOWNARIS,[1,6] KYLE A. REEVES,[1,7] AND ALLISON M. VISSICHELLI[1,8]

[1]*Environmental Studies Department, Gettysburg College, Gettysburg, Pennsylvania 17325 USA*
[2]*Università di Pisa, Dipartimento di Biologia, Unità di Biologia Marina e Ecologia, Via Volta 6, 56126 Pisa, Italy*
[3]*Mathematics Department, Frederick Community College, Frederick, Maryland 21702 USA*

Citation: Commito, J. A., A. E. Commito, R. V. Platt, B. M. Grupe, W. E. Dow Piniak, N. J. Gownaris, K. A. Reeves, and A. M. Vissichelli. 2014. Recruitment facilitation and spatial pattern formation in soft-bottom mussel beds. Ecosphere 5(12):160. http://dx.doi.org/10.1890/ES14-00200.1

Abstract. Mussels (*Mytilus edulis*) build massive, spatially complex, biogenic structures that alter the biotic and abiotic environment and provide a variety of ecosystem services. Unlike rocky shores, where mussels can attach to the primary substrate, soft sediments are unsuitable for mussel attachment. We used a simple lattice model, field sampling, and field and laboratory experiments to examine facilitation of recruitment (i.e., preferential larval, juvenile, and adult attachment to mussel biogenic structure) and its role in the development of power-law spatial patterns observed in Maine, USA, soft-bottom mussel beds. The model demonstrated that recruitment facilitation produces power-law spatial structure similar to that in natural beds. Field results provided strong evidence for facilitation of recruitment to other mussels—they do not simply map onto a hard-substrate template of gravel and shell hash. Mussels were spatially decoupled from non-mussel hard substrates to which they can potentially recruit. Recent larval recruits were positively correlated with adult mussels, but not with other hard substrates. Mussels made byssal thread attachments to other mussels in much higher proportions than to other hard substrates. In a field experiment, mussel recruitment was highest to live mussels, followed by mussel shell hash and gravel, with almost no recruitment to muddy sand. In a laboratory experiment, evenly dispersed mussels rapidly self-organized into power-law clusters similar to those observed in nature. Collectively, the results indicate that facilitation of recruitment to existing mussels plays a major role in soft-bottom spatial pattern development. The interaction between large-scale resource availability (hard substrate) and local-scale recruitment facilitation may be responsible for creating complex power-law spatial structure in soft-bottom mussel beds.

Key words: fractal power-law; Maine; mussel beds; *Mytilus edulis*; recruitment facilitation; self-organization; soft-bottom; spatial pattern.

Received 24 June 2014; revised 3 September 2014; accepted 4 September 2014; final version received 7 November 2014; **published** 23 December 2014. Corresponding Editor: D. P. C. Peters.

[4] Present address: Scripps Institution of Oceanography, University of California, La Jolla, California 92093 USA.

[5] Present address: Office of Protected Resources, National Marine Fisheries Service, National Oceanographic and Atmospheric Administration, Silver Spring, Maryland 20910 USA.

[6] Present address: Institute for Ocean Conservation Science, School of Marine and Atmospheric Sciences, Stony Brook University, 100 Nicholls Road, Stony Brook, New York 11794-5000 USA.

[7] Present address: Cashman Dredging & Marine Contracting Co., LLC, 549 South Street Quincy, Massachusetts 02269 USA.

[8] Present address: American University Washington College of Law, 4801 Massachusetts Avenue NW, Washington, D.C.

20016 USA.
† **E-mail:** jcommito@gettysburg.edu

Introduction

The processes that regulate landscape-scale pattern formation of organisms in terrestrial, freshwater, and marine systems remain poorly understood. In the marine realm, soft-bottom habitats cover nearly two-thirds of the earth's surface and have enormous ecological and economic importance. In these often relatively featureless sedimentary environments, soft-bottom mussel beds (*Mytilus edulis*) can form large, spatially complex aggregations with high biomass and energy flow (Commito and Dankers 2001, Commito et al. 2006, Crawford et al. 2006, van de Koppel et al. 2008, Gutiérrez et al. 2011). They are common in intertidal and shallow subtidal habitats at temperate and boreal latitudes, primarily in the northern hemisphere, and can cover as much as 8% of the surface of some tidal flats (Folmer et al. 2014). Mussels have high value as a commercial fishery and are ecosystem engineers that provide useful ecosystem services because they attenuate storm surge, stabilize the shoreline, sequester carbon, and provide food and habitat for many species (Commito et al. 2005, 2008, Bouma et al. 2009, Gutiérrez et al. 2011, Donadi et al. 2013).

Many factors can influence soft-bottom mussel bed spatial structure. For example, some mussel beds in northern Europe exhibit wave-like bands, which may arise from density-dependent positive (reduced rates of loss, increased phytoplankton delivery) and negative (food competition) interactions operating at different spatial scales at open, high-energy sites with flat bottoms and consistent water flow (Gascoigne et al. 2005, van de Koppel et al. 2005, 2008, Wang et al. 2009, Liu et al. 2012, van de Koppel et al. 2012). However, these factors may not be as important at other locations, where soft-bottom mussel beds occur in protected, low-energy sites with irregular shorelines and uneven bottom topography. In eastern Maine, USA (Fig. 1), mussel beds do not exhibit banded structure. They have power-law spatial distributions consisting of a hierarchical array of many sizes of interconnected, irregularly-shaped mussel patches containing open gaps (Fig. 2; Commito et al. 2006, Gutiérrez et al. 2011). Fractal analysis is well established in landscape ecology as a useful way to quantify such complex, hierarchical spatial patterns, where fractal dimension represents the power-law exponent (Hastings and Sugihara 1993, Halley et al. 2004, Crawford et al. 2006). Maine mussel beds exhibit fractal (i.e., power-law) patterning over gradients of density and percent cover (Snover and Commito 1998, Commito and Rusignuolo 2000, Crawford et al. 2006). Power-law structure has also been demonstrated for *M. edulis* at soft-bottom locations in northern Europe (Azovsky et al. 2000, Kostylev and Erlandsson 2001). This type of patchiness seems characteristic of soft-bottom beds (McGrorty et al. 1993, Nehls and Thiel 1993, Stillman et al. 2000, Commito and Dankers 2001, Dankers et al. 2001).

Soft-bottom mussel beds are fundamentally different from those on rocky shores because larval, juvenile, and adult mussels do not typically attach to the primary substrate, i.e., fine-grained sediment (Maas Geesteranus 1942, Bayne 1964, Commito 1987, Commito et al. 2005). Mussel abundance is negatively correlated with silt-clay content (Commito et al. 2008), and young mussels in particular are negatively correlated with substrate softness (McGrorty et al. 1993, Stillman et al. 2000). Mussel larvae, juveniles, and adults overwhelmingly attach to patches of hard substrate on the sediment surface, including other live mussels, shell hash (empty shells and shell fragments), and terrestrially derived pebbles and cobbles (McGrorty et al. 1993, Stillman et al. 2000, Dolmer and Frandsen 2002, Herlyn et al. 2008, wa Kangeri et al. 2014). If dislodged, mussels may be moved passively by water currents or actively crawl towards each other to re-establish at other mussel patches or create new patches (Maas Geesteranus 1942, Reusch and Chapman 1997, Côté and Jelnikar 1999, de Vooys 2003, Nicastro et al. 2007, van de Koppel et al. 2008, de Jager et al. 2011, Capelle et al. 2014).

Power-law structure can result from disturbance and recovery dynamics leading to criticality in wave-swept rocky shore mussel beds and other ecological systems (Wootton 2001, Guichard et al. 2003, Pascual and Guichard 2005).

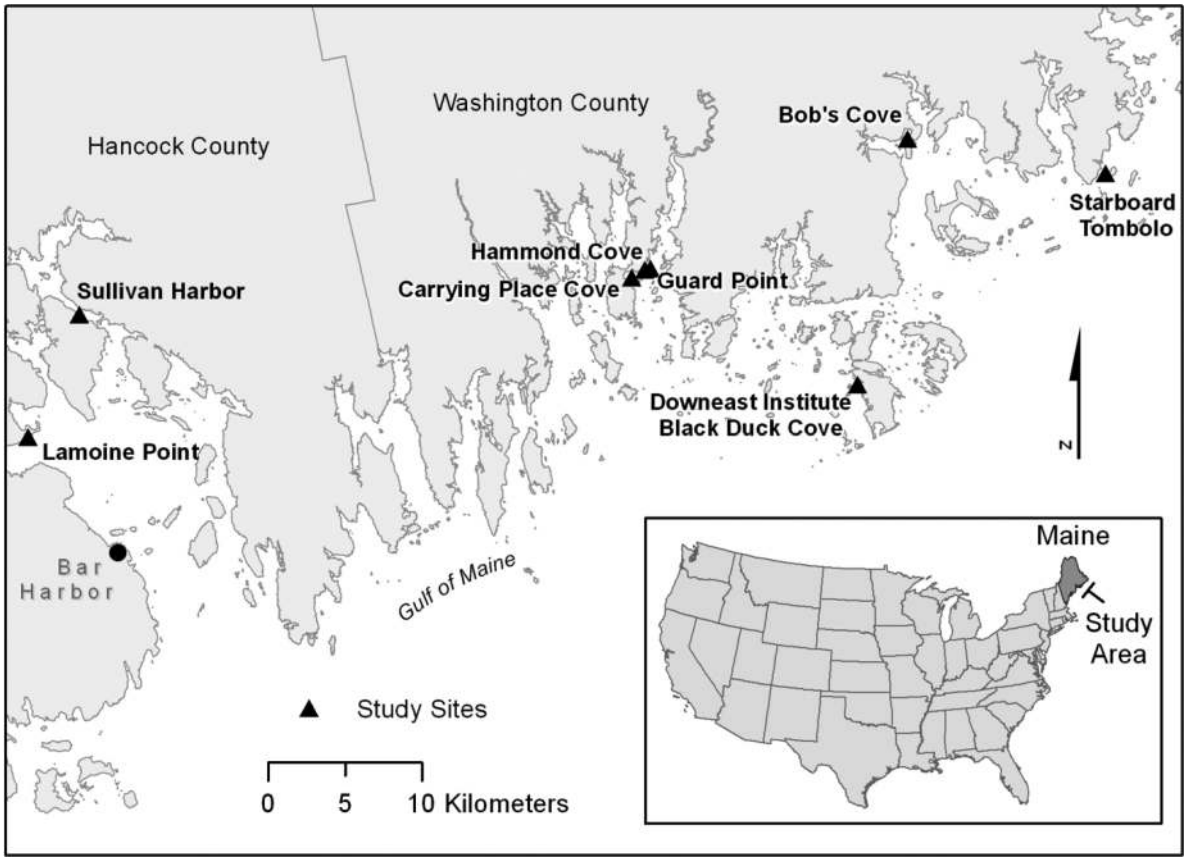

Fig. 1. Map of study sites in eastern Maine, USA.

However, not all systems with power-law structure are disturbance and recovery systems. Levin (1999) argued that in protected, low-energy locations, intrinsic factors should be important in regulating spatial structure of benthic organisms, resulting in power-law spatial distributions. We propose that recruitment facilitation is an intrinsic factor playing an important role in power-law spatial structure formation in mussel beds at soft-bottom locations like our research sites. We define recruitment facilitation as the preferential attachment of larval, juvenile, and adult mussels to existing mussel bed biogenic structure (especially live mussels) on or projecting above the sediment surface, as opposed to attachment to the surrounding fine-grained sediment and terrestrially derived pebbles and cobbles.

Power-law structure can emerge when a system grows by preferential recruitment to existing occupied sites (Barabási and Albert 1999). A well-known example is the power-law distribution of vegetation in arid ecosystems resulting from the interaction between large-scale resource constraints (water) and local-scale facilitation (seed dispersal and germination in moist soil adjacent to existing trees) in the absence of disturbance or any obvious criticality (Kéfi et al. 2007, Scanlon et al. 2007). Similarly, in a soft-bottom mussel bed system, the interaction between large-scale constraints (hard substrate available for attachment) and local-scale facilitation (larval, juvenile, and adult dispersal and attachment to existing live mussels) may create power-law patterning. Space is opened up by possible factors such as predators, storms, ice scour, or mortality from inadequate seston supply. As larval, juvenile, and adult mussels recruit, spatially complex beds grow out over the adjacent substrate, including sand and mud to which mussels do not attach. If this model of bed development is correct, then some mussels are

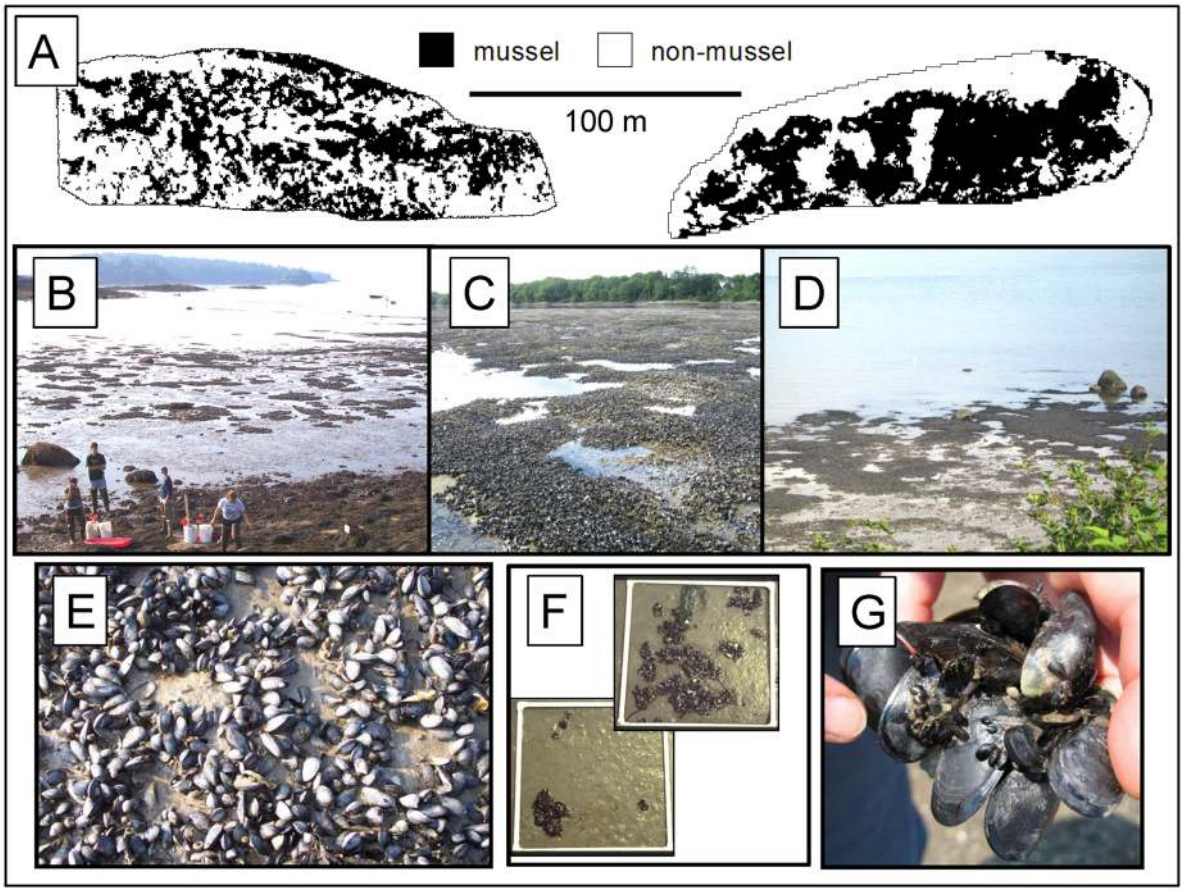

Fig. 2. Mussel bed images from eastern Maine, USA. (A) Entire beds at Sullivan Harbor (left) and Bob's Cove (right), adapted from Crawford et al. (2006), with kind permission from Springer Science + Business Media; (B, C, D) portions of study site beds at intermediate spatial scale (left to right panels are Guard Point, Sullivan Harbor, and Guard Point, respectively), (E, F) bed patchiness at small spatial scale (quadrats = 0.5 × 0.5 m; left to right panels are Hammond Cove and Sullivan harbor, respectively), (G) small mussels attached to clump of large individuals at Guard Point. Photos credit: J. A. Commito.

attached to gravel and shell hash, but most are attached to other mussels.

In this paper we present results from a simple lattice model that demonstrate how facilitation of recruitment to existing mussels produces fractal power-law patterns like those observed in real beds in Maine. We then present results from field sampling and field and laboratory experiments guided by the model to test hypotheses regarding mussel recruitment. The results support the idea that facilitation of recruitment to existing mussels plays a major role in creating complex power-law spatial patterns in soft-bottom mussel beds.

Methods

Study area

Our research focuses on a 70-km (Euclidean distance) stretch of the coast (44°31′36″ N, 68°14′10″ W to 44°36′03″ N, 67°23′36″ W) in Hancock and Washington counties, eastern Maine, USA (Fig. 1). The glaciated, highly dissected shoreline creates a complex array of intertidal flats that are the spatially dominant feature of this coastal region. Embayments and estuaries are relatively protected from wind-generated currents and waves by the hilly, forested mainland, peninsulas, and islands. *Mytilus edulis* and *M. trossulus* can live together

with their hybrids, but at protected and estuarine sites in eastern Maine, the overwhelming majority of individuals are *M. edulis* (Riginos and Cunningham 2005, Hayhurst and Rawson 2009, Tam and Scrosati 2014). The sediment is most often mud or muddy sand with a flat, unrippled surface, indicating a low-energy environment of slow wind- and tide-generated current velocities. Terrestrially derived pebbles, cobbles, and boulders resulting from glacial activity generally represent a small percentage of bottom cover. The rocky shore in these locations is dominated by the alga *Ascophyllum nodosum*, an indicator of slow current velocities and low to moderate wave activity (Bertness et al. 2002). Mussel dislodgement rates by storms and ice scour are relatively low in low-energy, soft-bottom estuaries and embayments (McGrorty et al. 1990, Hamilton et al. 1999, Stillman et al. 2000, Brinkman et al. 2002, Belt et al. 2009). Sites in Maine protected enough for soft-bottom mussel beds generally have soft, wet winter slush that is unlikely to be an important disturbance agent (J. A. Commito, *personal observation*; B. F. Beal, *personal communication*). Potential mussel predators at our soft-bottom sites include dog whelks (*Nucella lapillus*) and green crabs (*Carcinus maenas*), both at lower densities than on rocky shores (Commito et al. 2008), and eiders (*Somateria mollissima*), which are typically at rocky intertidal sites and shallow subtidal kelp beds and sea urchin barrens rather than soft-sediment locations (Guillemette and Himmelman 1996, Hamilton 2000).

Fractal dimensions (D) can range from 1 for a simple Euclidian shape to 2 for a shape so complicated that a trace of its outline fills the entire plane. Mussel beds at our sites exhibit fractal power-law patterning at scales ranging from 2.5 mm to 200 m, nearly five orders of magnitude. For small quadrats, an open-downward parabolic relationship exists between fractal dimension and mussel percent cover, with highest D values around 60% cover (Snover and Commito 1998, Crawford et al. 2006). Percolation theory predicts the establishment of a percolation cluster at approximately 60% cover (Guichard et al. 2003, Scanlon et al. 2007), beyond which the empty gaps fill in to such an extent that the pattern becomes less complex and D decreases. At larger spatial scales, D values similar to the values for individual quadrats were calculated for two entire mussel beds, each approximately 200×50 m (Crawford et al. 2006).

Mussel bed recruitment facilitation model

We tested the hypothesis (H_1) that mussel bed development in a lattice model with facilitation of recruitment to live mussel substrate produces power-law spatial structure similar to that observed in Maine soft-bottom mussel beds. Lattice models have been used successfully to describe the spatial dynamics of rocky shore mussel beds and other ecological systems (Wootton 2001, Guichard et al. 2003, Pascual and Guichard 2005, Kéfi et al. 2007, Scanlon et al. 2007). In our model, mussel bed cover grows continuously by the addition of new mussels to the edges of existing mussel patches. Although extremely simple, the model mimics what is known about mussel recruitment in nature, where recent larval recruits are found primarily at the edges of mussel patches (Svane and Ompi 1993), and crawling juvenile and adult mussels attach there as well (Maas Geesteranus 1942, Côté and Jelnikar 1999, de Vooys 2003, Nicastro et al. 2007, van de Koppel et al. 2008, de Jager et al. 2011).

The model mussel bed was represented by a square lattice of 100×100 cells (Visual Basic 6.0 1999; see Appendix A for full description of the model and Supplement for source code and executable file with interface for readers to use). The borders were not wraparound, and each cell had at most four orthogonal neighbors (von Neumann neighborhood). Cells were in either the empty state or the filled state, representing absence or presence of a mussel, respectively. No distinction was made among larval, juvenile, and adult mussels. After an initial random assignment of mussel-filled "recruitment site" cells, the lattice was updated asynchronously. One cell was chosen at random. If the chosen cell was already filled, it remained filled. If it was empty and had no filled neighbors, it remained empty. If it was empty and had at least one filled neighbor, it became filled. This scenario represents the attachment of recruits to the edges of mussel patches, including the edges of interior gaps, causing an increase in bed cover. The number of starting recruitment sites, number of iterations, and pattern of recruitment input (i.e., random or

spatially structured) could be varied, and the model could also allow mussel removal from filled cells, as well as recruitment to cells not adjacent to filled cells. For the purposes of this investigation, we kept the recruitment facilitation scenario as simple as possible. We used a range of initial recruitment site densities, and recruits entered the lattice at random as described above, without removal. Each initial recruitment site density was run with five different random distributions, an adequate number because model output variability was low.

For all model output images, the fractal dimension was calculated with the boundary-grid method using Benoit 1.3 software (TruSoft 2004). The number of grid boxes entered by a mussel patch outline was plotted against grid box side length using log-log axes, and fractal dimension D = the negative of the slope value. The number of filled cells was also noted. In order to make accurate comparisons between the model and previously published field results from Maine, the images in Snover and Commito (1998) and Crawford et al. (2006) were re-analyzed with the same procedure utilized for the model output images. We used three criteria to assess model results. To accept the hypothesis, the model had to produce: (1) spatially complex arrays of irregularly shaped mussel patches and gaps with a wide range of sizes; (2) fractal dimension values similar to those observed for mussel beds in the field ($D = 1.15$–1.40); and (3) a downward-opening parabolic relationship between fractal dimension and percent cover, with a peak at approximately 60% cover.

Observations and experiments on relationships between mussels and hard substrate in the field

We tested the hypothesis (H_2) that mussels preferentially recruit to live mussel biogenic structure, compared to fine sediment, terrestrially derived pebbles and cobbles, and mussel shell hash. We used a combination of field observations and a field experiment.

Spatial scales of variability for mussels and hard substrate.—Mussel abundance is highly variable at our research sites: mean ± 1 SE = 23.52 ± 7.47 individuals/200 cm^2 core; range = 0–958 individuals/200 cm^2 core (Commito et al. 2006). In that study, the highest proportion of variation in abundance of recent mussel recruits and total mussels was at small spatial scales, i.e., <10 m.

To obtain comparable data on spatial variation in coarse sedimentary hard substrates to which mussels can potentially recruit (i.e., terrestrially derived gravel, mussel shell hash, and non-mussel shell hash), sediment was utilized from stored bottom samples collected originally at six sites (Fig. 1) by Commito et al. (2006), where complete details can be found. Briefly, mussel beds were sampled with a nested regime of cores (20 cm tall × 16 cm diameter = 200 cm^2 cross-sectional area, 4021 cm^3 volume) within quadrats (1 m^2) within transects (6 m long) within positions (from a 120 m wide band running down the center of each bed from the upper to lower bed margin, approximately 100 m at each site) within sites (spread out along 70 km Euclidean distance of the coast). Each nested level in the design represented a larger spatial scale in terms of lag, or distance between sampling units (Dungan et al. 2002).

For the coarse sediment (>8 mm) analysis required in this investigation, the archived sample material was air dried and sieved on a shaker through a graded series of mesh sizes. The material was separated into three categories and weighed: terrestrially derived pebbles and cobbles called "gravel" for simplicity; mussel shell hash; and non-mussel shell hash. This material is not a perfect measure of the coarse substrate to which mussels can attach because it includes both surface and buried material. However, fine-grained sediment moves across the surface with every tidal cycle (Commito and Tita 2002, Commito et al. 2005), potentially covering and exposing coarse material on a daily basis, so a measurement of surface availability at any one point in time may not be particularly useful. In our field experience, the mass of total coarse material is generally correlated with the mass of surface coarse material and serves as an adequate proxy.

Data were analyzed with a pure random effects (Model II) nested-ANOVA (Sokal and Rohlf 1995, Underwood 1997) using the Statistix 8 analysis package (Analytical Software 2003). A test of global Moran's I using GeoDa (Anselin 2003) revealed that all independent variables demonstrated significant spatial autocorrelation at the $P < 0.05$ level, as we expected for such a

spatially aggregated system. Furthermore, independent variables were heteroscedastic and far from normally distributed even when transformed. Although this situation violates the assumptions of traditional hypothesis testing, it does not influence parameter estimation (Underwood 1997) or Pearson correlation coefficients (Haining 1990). Our goal was to compute the proportion of total variance accounted for at each level in the nested design, so we proceeded with the analysis, as recommended by Benedetti-Cecchi (2001) and Bishop et al. (2002). In nested-ANOVA studies it is often the case that variability at a given spatial scale is less than predicted from the amount of variability found at a smaller scale, resulting in a negative estimate of variance. When this situation occurred, we followed the "pool-the-minimum-violator" procedure recommended by Fletcher and Underwood (2002).

Correlations between mussels and hard substrate.—To determine the relationships between mussel abundance and hard substrate, Pearson correlations were calculated with Statistix 8 (Analytical Software 2003) between log-transformed mussel abundance and hard substrate mass in each category from the samples described above.

Mussel attachment to hard substrate.—To determine the types of hard substrate to which mussels were actually attached, individuals were examined 20–22 July 2006 at three beds chosen from the six beds described above to represent a wide range of substrate availability (details in Commito et al. 2006, Commito et al. 2008). Lamoine Point is relatively exposed with more coarse sediment material than the other two sites. Sullivan Harbor and Bob's Cove are relatively protected sites with a mix of fine and coarse sediment types.

At each bed, three 10-m transects were established parallel to the shoreline, one each in the high, middle, and low intertidal zone. Samples were collected from mussel patches >15 cm in diameter. Each sample consisted of all the mussels found within a 10.5 cm diameter metal ring pushed 3 cm into the sediment to the bottoms of the mussels and the substrate to which they were attached. From four to eight samples were taken along each transect, depending on the numbers of mussels obtained, for a total of 16 samples per site. Mussel clumps were gently rinsed in situ with seawater on 0.5-mm mesh, and the number of substrate categories to which each mussel was attached by its byssal threads was determined, using a hand lens when necessary. Attachment categories included: live mussels; mussel shell hash; non-mussel shell hash (primarily plate fragments of the barnacle *Semibalanus balanoides* and shell fragments of the clams *Mya arenaria* and *Macoma balthica*); terrestrially derived material defined as pebbles (<1 cm diameter), small cobbles (1–5 cm), and large cobbles (>5 cm); live barnacles; and dead barnacles. The live and dead barnacles were almost always cemented to live mussels, mussel shell hash, and gravel, covering a small area of those surfaces. The frequencies of mussel attachment were calculated across categories.

Mussel recruitment to hard substrate.—An experiment to measure mussel recruitment to a variety of substrate types was conducted at three mussel bed sites. Guard Point and Hammond Cove (both in the six sites described above) and nearby Carrying Place Cove (Fig. 1) are in protected embayments with muddy sand bottoms. At each site, 10 mussel patches were selected based on patch size (>2.5 m in minimum dimension), location (as close to random as possible in the lower intertidal while also being >5 m apart), and orientation (so that experimental blocks faced random compass directions).

Experimental blocks were established 3–5 July 2007. Each block (Fig. 3) consisted of four randomly placed recruitment substrate plots (live mussels, mussel shell hash, gravel, and muddy sand) and an ambient core, each in two habitats (mussel patch and bare sediment). Larval, juvenile, and adult mussels are sensitive to surface roughness, chemical compounds, and metal ions, so plots consisted of substrates held in food-grade plastic delicatessen containers with a smooth, shiny surface and rim, 10.5 cm in diameter and 4.5 cm deep, with holes drilled for drainage. At low tide they were filled with substrates taken from each site, respectively. Substrate plots were deployed 25 cm from each other and from the edge of the mussel patch. They were placed into the bottom where sediment and mussels had been removed to create holes of the same diameter and depth as the containers. Container rims were flush with the

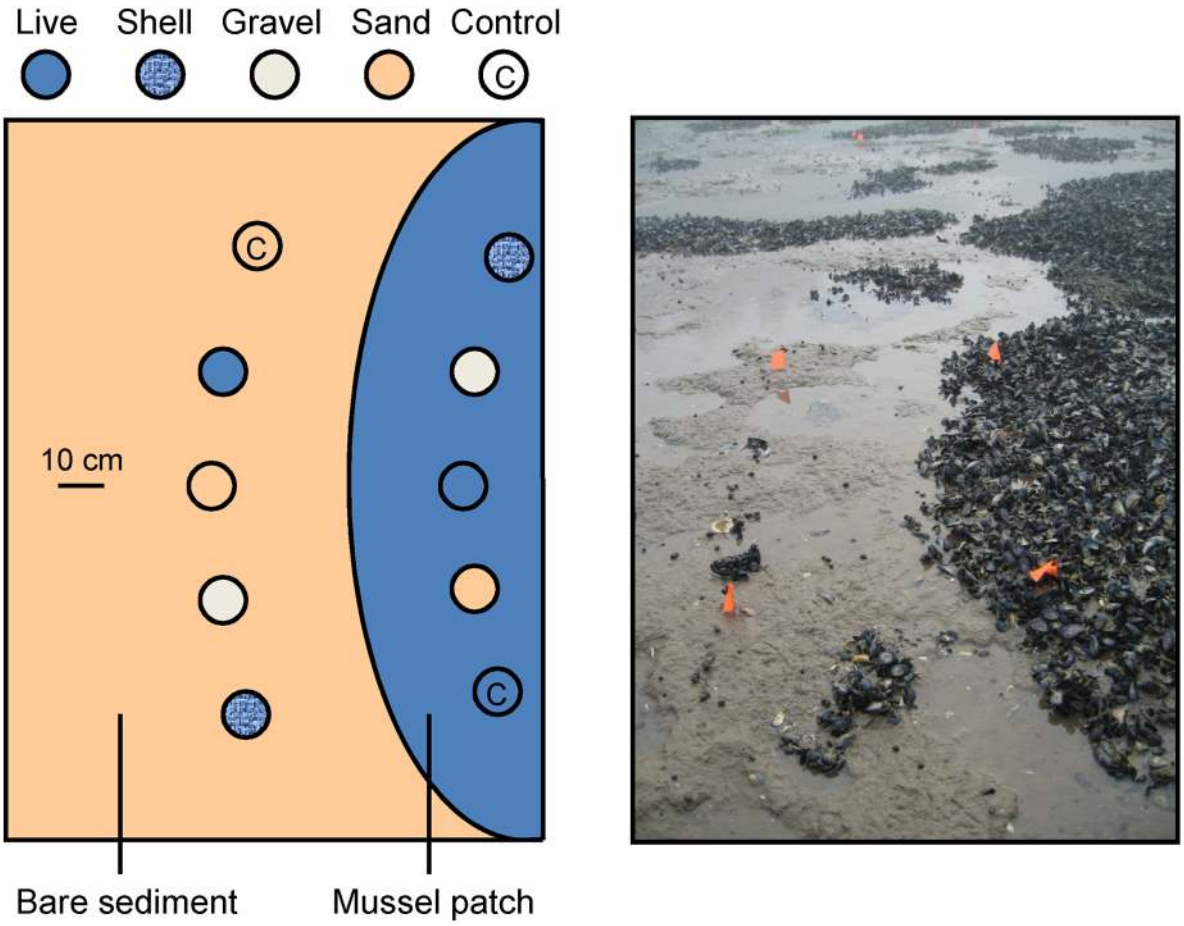

Fig. 3. Diagram and photograph of recruitment experiment block at Hammond Cove, Maine. Photo credit: J. A. Commito.

bed surface and held in place with plastic-covered wire hooks. Ideally, the live mussels would have been marked to differentiate them from recruits. However, the standard methods of marking bivalves involve notching the shell margin or cleaning a portion of the shell and applying paint or gluing on a tag. All were deemed unacceptable for an investigation of recruitment because of the possible release of chemical cues from injured mantle tissue, alteration of the shell surface, or leaching of chemical solvents. Instead, the live mussel plots were created with individuals >25 mm long, and recruits in all treatments were the mussels <25 mm long found in the plots and cores at the end of the experiment.

Four weeks later (3–5 August 2007) the substrate plots were removed and ambient cores of the same diameter and depth were taken. The contents were placed into plastic bags with buffered formalin and stained with Rose Bengal. In the laboratory the samples were sieved on 250-μm mesh. All mussels were removed and the lengths measured to the nearest 0.1 mm.

Data were analyzed with ANOVA using the Statistix 8 analysis package (Analytical Software 2003), where the randomized blocks and the interactions involving blocks were nested within Sites, and the fixed factors of site, habitat, and substrate were orthogonal to each other. The data did not meet the necessary criteria for ANOVA, even when transformed. Following Zar (1999), the data were globally ranked, and the analysis was run on the ranked data as well as the original data. Especially in balanced designs like ours with no missing data, this procedure produces a

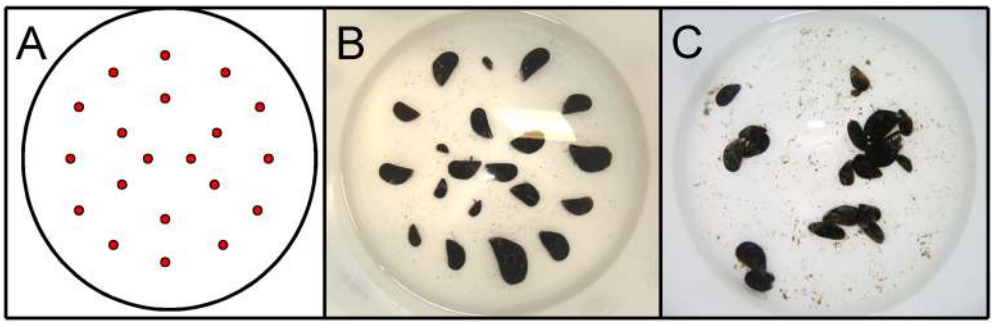

Fig. 4. Arenas for aggregation experiment in the laboratory at Downeast Institute for Applied Research and Education, Black Duck Cove, Great Wass Island, Maine. Arena diameter = 25 cm, (A) Twenty evenly spaced mussel placement locations, (B) mussels in place at time = 0, foot emerging from two mussels near left-center of the array, (C) mussels in clumps after 24 h. Photos credit: J. A. Commito.

dependable result when both analyses yield the same conclusion (Zar 1999). Significant differences were examined further with Tukey's multiple comparison procedure at a rejection level of $\alpha = 0.05$.

Mussel aggregation laboratory experiment

We tested the hypothesis (H_3) that juvenile and adult mussels recruit by crawling towards each other, self-organizing into aggregations with power-law spatial structure. A laboratory experiment to assess juvenile and adult mussel movement was conducted at the Downeast Institute for Applied Research and Education, Black Duck Cove, Great Wass Island (Fig. 1). Mussels were collected at low tide 16 July 2007 from a natural mussel bed at Black Duck Cove. Mussel clumps were gently removed from the substrate, placed in flowing seawater (filtered through 750 μm mesh) in the laboratory for a 24-h acclimation period, and placed into size classes: small (5.0–19.9 mm), medium (20.0–29.9 mm), and large (30.0–39.9 mm).

Mussel aggregation test arenas consisted of 18.93 L (5 U.S. gallons), 25 cm diameter, white, plastic buckets with smooth, featureless interiors. Test arenas were filled with seawater for 24 h to condition them before use and then emptied. For the experiment, 2 L of seawater was added to each of eight test arenas at 1400 hrs on 17 July. The temperature of the arena water was 17.0°C, similar to water temperatures recorded at Black Duck Cove (18.0–24.5°C, sunny, mid-day, 10–50 cm deep near low tide line). Twenty mussels were placed on the bottom of each arena in a radially symmetrical pattern, with mussel centers 3.5 cm equidistant from each other in concentric circles and their narrow ends facing the center (Fig. 4). Five small, 10 medium, and five large mussels were used to simulate the frequency distribution in the field. Mussel positions were randomized across size classes. Because mussels began to move within seconds, it was not possible to take photographs of the initial conditions in a timely manner while the eight arenas were being set up. To have an initial condition baseline, we set up three additional arenas at the same time as the test arenas, specifically for the purpose of photographing the 20 mussels as soon as they were placed into position. During the experiment, the laboratory's fluorescent lights were turned on at 0730 hrs and turned off at 1600 hrs. Natural light entered the room through numerous windows. Sunset on 17 July occurred at 2011 hrs, sunrise on 18 July occurred at 0501 hrs, and the lunar cycle was at a new moon.

Arenas were left undisturbed for 24 h, when a digital photograph was taken of the bottom of each arena. Mussel aggregations were categorized in situ by two methods: shells physically touching and individuals connected by byssal thread attachment. Both methods yielded almost identical results, so for simplicity the results are reported here only for the shell-touching data. The number of aggregations/arena and the number of mussels/aggregation were recorded. An aggregation was defined as a clump containing two or more mussels (following Côté and Jelnikar 1999).

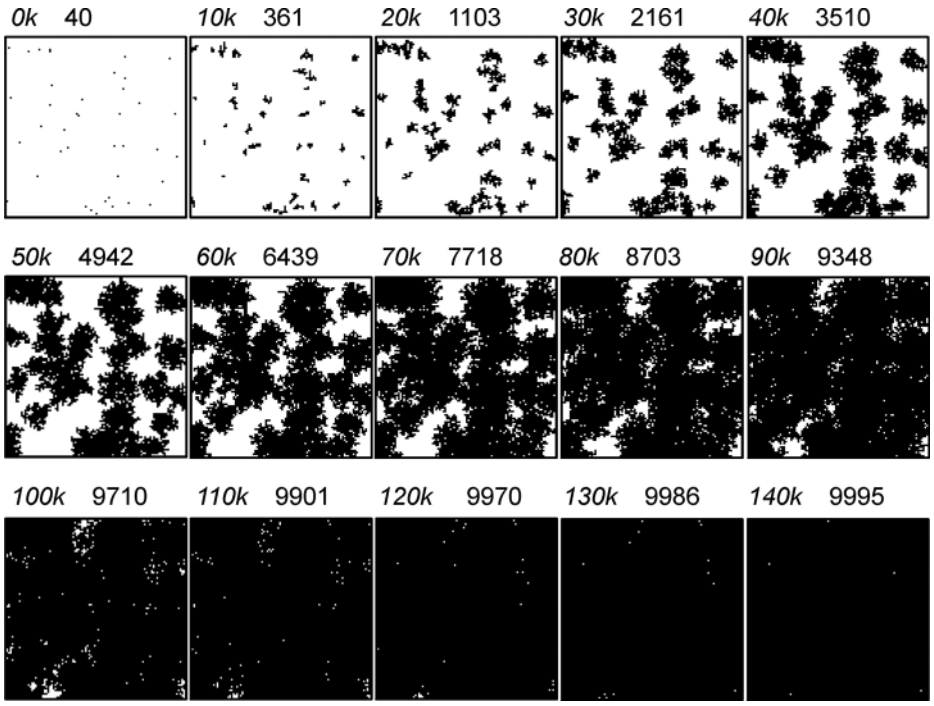

Fig. 5. Example of model mussel bed development from 40 randomly located initial recruitment sites in a $100 \times 100 = 10{,}000$ cell lattice. Numbers above panels refer to iterations (in thousands) and filled cells, respectively.

The digital photographs were used to determine fractal dimensions (D) and perimeter (P), area (A), and perimeter:area (P:A) ratios of mussel singletons and aggregations. Photographs were transformed for analysis using ArcGIS 9.2 software (Environmental Systems Research Institute 2006). Mussel outlines were signified with a one-pixel white boundary on a black background. Perimeters and areas were calculated using the geometry calculator of ArcGIS 9.2. The Mann-Whitney *U*-test (SPSS 2006) was used to compare P:A values of aggregations to those of singletons as well as entire arenas after 24 h to those under initial conditions.

To determine fractal power-law patterns for the shapes of individual aggregations, the boundary-grid method was utilized with Benoit 1.3 software (TruSoft 2004). Because of the large number of single mussels, which were similar in shape, 20 singletons were chosen at random for analysis. The Mann-Whitney *U*-test was used to compare fractal dimension values of aggregations to those of singletons.

To determine arena-wide power-law clustering, the area-perimeter exponent technique was used (Hastings and Sugihara 1993), where aggregation P and A values were plotted on log-log axes for each arena, and fractal dimension $D = 2 \times$ slope. We chose this method for the arena-wide analysis because it was developed specifically for clusters of patches (as opposed to quadrats or individual patches), and other work in our laboratory demonstrated that it is more sensitive than the boundary-grid method to differences in arena cluster patterns (N. J. Gownaris, D. E. Haulsee, S. E. Coleman, and J. A. Commito, *unpublished data*). The Mann-Whitney *U*-test was used to compare fractal dimension values of arenas after 24 h to those under initial conditions.

Results

Mussel bed recruitment facilitation model

The model showed the accumulation of recruits at the edges of mussel patches, including edges of interior gaps, causing growth in bed cover (Fig. 5). Bed growth was rapid at first and slowed down as the number of open cells along

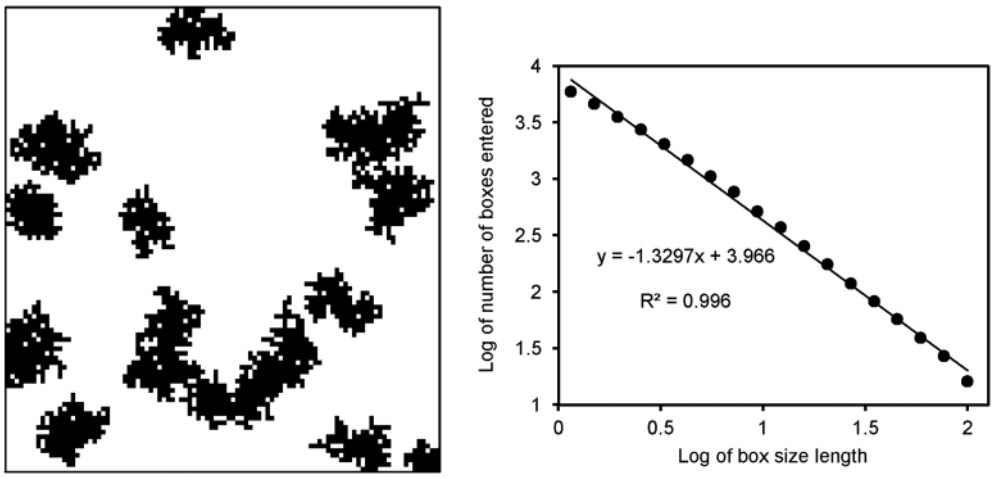

Fig. 6. Example of recruitment facilitation model run with 20 initial recruitment sites and growth to 20% cover and the associated power-law graph. "Box" refers to grid boxes in boundary-grid method used to calculate fractal dimension, *D*.

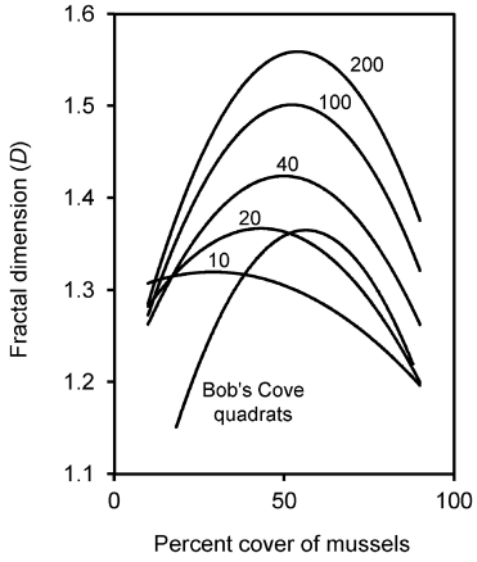

Fig. 7. Fractal dimension, *D*, of mussel outline vs. percent cover of mussels. Second order regression curves are for model mussel beds with the indicated numbers of initial recruitment sites and for the Bob's Cove, Maine, mussel bed quadrats in Snover and Commito (1998) and Crawford et al. (2006), recalculated using the same image analysis methodology as for the model runs. See Appendix B: Fig. B1 for the curves with regression equations, coefficients of determination, and data points.

edges declined, causing fewer recruitment sites to be available. Qualitatively, the hierarchical spatial structure that emerged was visually similar to what was observed in the natural beds at our study sites (compare to Fig. 2). Patches were irregular in shape, with empty gaps within and between patches. Mussel removal was not part of the model scenario, yet gaps were prominent features. Gaps were created in two ways – when irregular evaginations grew out from a patch edge and encircled open spaces within the patch and when two or more patches grew towards each other and coalesced.

Quantitatively, the model produced power-law spatial patterns like those of mussel beds in the field (Fig. 6). The model fractal dimension values were slightly higher, which was not unexpected because small, consistent differences may result from differing types of source data. Fractal dimension exhibited the same downward-opening parabolic relationship with percent cover (Fig. 7; see Appendix B: Fig. B1 for expanded version with data points and regression equations) reported for Bob's Cove quadrats (Snover and Commito 1998, Crawford et al. 2006). Depending on the number of initial mussel recruitment sites, a family of these parabolic curves was produced. With small numbers of initial mussel recruitment sites, the curves were relatively flat. As the number of initial mussel recruitment sites increased, the variability de-

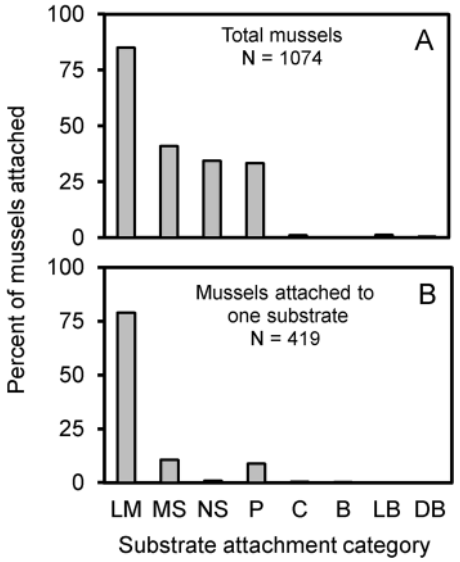

Fig. 8. Mussel attachment to hard substrate at mussel beds in eastern Maine, USA. (A) Total mussels attached to all substrate categories, which add up to more than 100% because mussels may be attached to more than one substrate category, (B) mussels attached to one substrate category. Substrate categories: LM = live mussels, MS = mussel shell hash, NS = non-mussel shell hash, P = pebbles, C = cobbles, B = boulders, LB = live barnacles, DB = dead barnacles.

clined, parabolas became more strongly arched, *D* values rose, and peak values shifted to the right. As expected from percolation theory and the Bob's Cove empirically derived parabola, they were highest around 60% cover. Thus, density of initial recruitment sites as well as overall percent cover played important roles in spatial patterning.

Observations and experiment on relationships between mussels and hard substrate in the field

Spatial scales of variability for mussels and hard substrate.—Hard substrate in the form of coarse sediment was highly variable (mean ± 1 SE = 458.23 ± 46.66 g/core; range = 0–3404.83 g/core). It consisted primarily of terrestrially derived gravel (80.9%), followed by far smaller amounts of mussel shell hash (16.0%) and non-mussel shell hash (3.0%). Variance for all coarse sediment types was highly dependent on spatial scale. For the dominant category (terrestrial gravel), the highest proportion of the variance (54.95%) occurred at the largest spatial scale (kilometers, the site level), and the lowest proportion (2.41%) was at the second-smallest spatial scale (<10 m, quadrat level). Corresponding values were similar for total coarse sediment: 51.72% at the largest spatial scale and 1.67% at the second-smallest scale. This pattern was the opposite of the one for mussels at the same locations: highest variance (44.03%) at the second-smallest scale and lowest variance (3.80%) at the largest scale (Commito et al. 2006). Although mussels and potential attachment substrate were both hierarchically structured, their structures differed considerably across spatial scales.

Correlations between mussels and hard substrate.—Recent larval recruits (<2 mm) had a significant positive correlation with only one type of hard substrate: adult mussels ($r = 0.298$, $P = 0.0003$). They were negatively correlated with non-mussel shell hash ($r = -0.284$, $P = 0.0006$) and not significantly correlated with the other coarse sediment substrates. Adult mussels and total mussels were not significantly correlated with any of the coarse sediment substrates.

Mussel attachment to hard substrate.—Attachments were assessed for 1074 mussels. Most mussels were attached to one or two substrate categories (mode = 1; median = 2; mean ± 1 SE = 1.97 ± 0.03; range = 1–5 substrate categories/mussel). Overall, 85.1% of the mussels were attached to other live mussels, more than twice as many as any other substrate category, followed by mussel shell hash, non-mussel shell hash, and small pebbles (Fig. 8A). Nearly all of the mussels (94.2%) were attached to biogenic structure in the form of either live mussels or mussel shell hash.

To the degree that mussel attachment reflects recruitment selectivity, it is useful to consider the mussels that were attached to only one substrate category. These individuals (N = 419) represented 39% of all mussels. Of this number, 79.0% were attached only to other live mussels, eight times as many as any other substrate category, and 89.7% were attached to biogenic structure in the form of either live mussels or mussel shell hash (Fig. 8B).

Mussel recruitment to hard substrate.—The ANOVAs on raw data and ranked data from the recruitment field experiment produced extremely similar results for all main effects and interactions, the single exception being signifi-

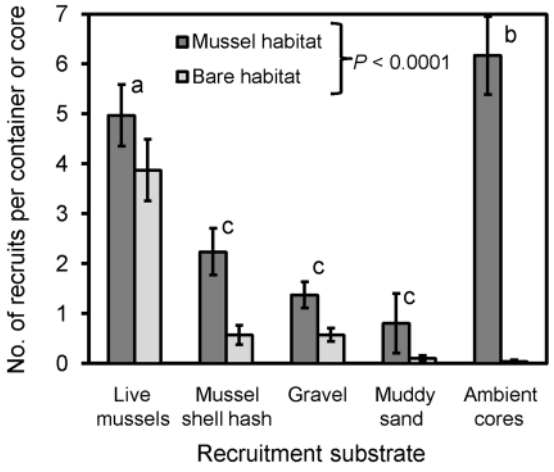

Fig. 9. Mussel recruits (mean ± 1 SE) in experimental substrate plots and ambient cores in mussel and bare sediment habitats at three sites in eastern Maine, USA. Plot and core diameter = 10.5 cm, depth = 4.5 cm. Letters indicate significant differences among substrates ($P \leq 0.05$). Mussel habitat had significantly more recruits than did bare sediment. No significant differences among sites. See Fig. 3 for diagram and photograph of experimental block and Appendix C: Tables C1, C2 for ANOVA table and Tukey HSD all-pairwise comparisons test results.

cant site differences for the ranked data but not for the raw data. We were not as interested in sites as in habitats and substrates, for which the analysis was deemed to be reliable.

The number of recruits was significantly higher in the live mussel substrate plots than in any of the other substrate plots, indicating a strong effect of substrate type (Fig. 9; see Appendix C: Tables C1, C2 for ANOVA and Tukey HSD all-pairwise comparisons results). The mussel shell hash, gravel, and muddy sand plots held progressively fewer recruits, but were not significantly different from each other. This pattern was the same in both the mussel and bare sediment habitats. In addition, the number of recruits was significantly higher in the mussel habitat than in the bare sediment habitat, demonstrating a strong effect of local, ambient mussels on recruitment.

The substrate × habitat interaction term was significant, as might be expected from the large difference in recruits between the ambient cores in the mussel and bare sediment habitats. The site × substrate interaction was also significant, indicating that recruitment patterns across sites were differentially affected by substrate. The numbers of recruits did not vary significantly across the three sites, suggesting that recruitment was occurring at similar rates over spatial scales encompassing more than single mussel beds.

Approximately 94% of the recruits were ≥2 mm, indicating that juveniles and adults were more important recruiters than larvae during the time of the experiment. No individuals <2 mm were found in any muddy sand plots or bare sediment control cores. Recruits within each substrate plot rarely occurred as isolated individuals spread out across the surface. They were almost always clumped together into one or a few aggregations/plot, attached by many byssal threads to each other as well as to the hard (but not the muddy sand) substrate types.

Mussel aggregation laboratory experiment

At the start of the laboratory experiment, mussels immediately began to crawl by extending the foot and pulling themselves along the bottom. Within the first minute, some mussels made shell contact or formed byssal thread attachments with each other. After a few minutes, aggregations were common. Mussels did not move solely as individuals. They pushed and pulled other individuals with them, creating mobile clumps. Aggregations often broke up and reformed during the first few hours, after which time they became relatively stable.

At the end of the experiment (see example in Fig. 4), about half of the 20 mussels in each arena were in aggregations (mean ± 1 SE = 10.63 ± 1.12 mussels/arena), with as many as 6 mussels/aggregation (Fig. 10A). Despite their irregular shapes, the large sizes of aggregations compared to singletons meant that they had significantly lower P:A ratios ($U = 434$, df = 73, 35, $P < 0.0001$; Fig. 10B).

As expected for smooth, simple shapes, the fractal dimension values ≈ 1 for individual mussels (Fig. 10C) and for initial condition arenas comprising 20 isolated individuals (Fig. 10D). Aggregations had shapes with significantly higher fractal dimensions than singletons ($U = 113$, df = 20, 34, $P < 0.0001$; Fig. 10C). Arenas after 24 h held aggregation clusters with significantly higher arena-wide fractal dimensions

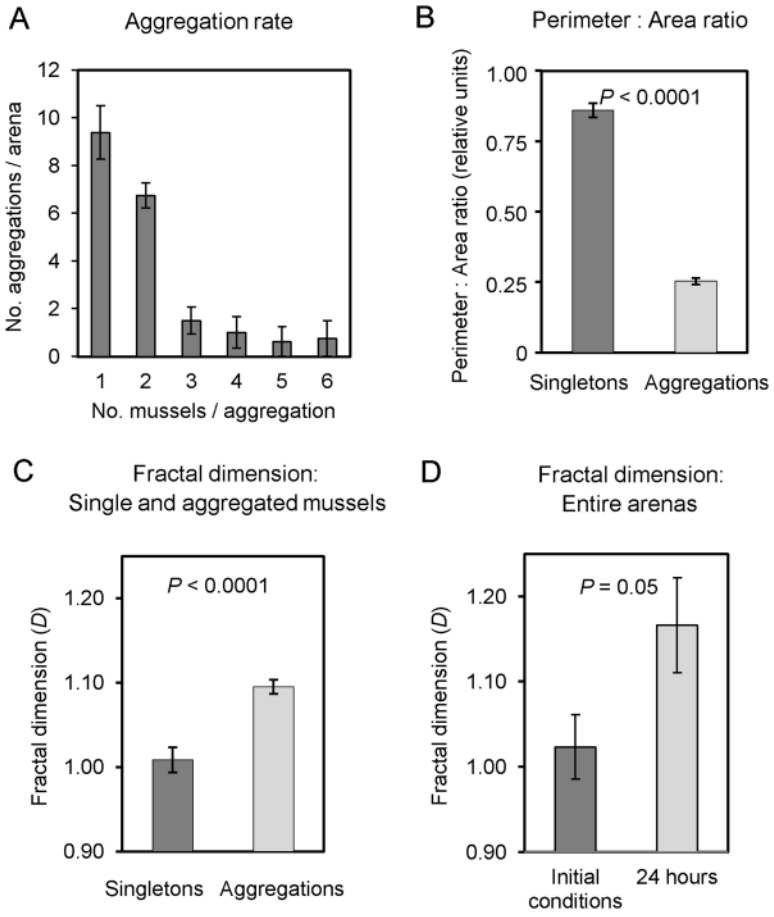

Fig. 10. Laboratory aggregation experiment results. (A) Aggregation rate as frequency distribution of mussels in aggregations (mean ± 1 SE), (B) perimeter:area ratios (mean ± 1 SE) of single mussels and mussel aggregations, (C) fractal dimensions (mean ± 1 SE) of single mussels and mussel aggregations, (D) fractal dimensions (mean ± 1 SE) of entire arenas.

than initial condition arenas ($U = 22$, df = 8, 3, $P = 0.05$; Fig. 10D). Thus, mussel movement created power-law spatial structure at the levels of individual aggregations and of entire arenas.

Discussion

Mussel bed recruitment facilitation model

Our lattice model scenario was designed to test the hypothesis (H_1) that the simplest recruitment facilitation rules could simulate Maine soft-bottom mussel bed power-law spatial structure without invoking a power-law array of gap sizes produced by disturbance agents incorporated in wave-swept rocky shore lattice models (Wootton 2001, Guichard et al. 2003, Pascual and Guichard 2005). In fact, our model produced gaps without any mussel removal. Our main heuristic outcome was that facilitation of recruitment to existing mussels caused irregular patch growth and coalescence on a sedimentary seafloor to which mussels cannot readily attach, producing patches and gaps with power-law structure. These patterning processes most likely contribute to the interconnected, labyrinth-like structures (sensu van de Koppel et al. 2008) often observed in soft-bottom mussel beds (Fig. 2; Snover and Commito 1998, Crawford et al. 2006, van de Koppel et al. 2008). Without recruitment facilitation, power-law spatial patterning may not occur. For example, a well-parameterized lattice model for New Zealand soft-bottom bivalves with high

rates of juvenile and adult movement failed to produce the patchy, spatially auto-correlated patterns observed in the field, which the authors (McArdle et al. 1997) attributed to the lack of recruitment facilitation in the model.

In their review of spatial self-organization in estuarine ecosystems, van de Koppel et al. (2012) suggested that fractal power-law structure at sites like ours in Snover and Commito (1998) is the result of storm disturbance breaking up banded patterns of young mussel beds during their first winter. However, for the past four decades at our sites we have never observed banded patterns of young mussels or mussels of any age, regardless of season. Of course mussel removal is important; it helps determine what hard substrate is available for mussel recruitment. Yet our model results were consistent with other power-law structured systems exhibiting recruitment facilitation in the absence of disturbance gaps (Barabási and Albert 1999, Kéfi et al. 2007, Scanlon et al. 2007). In fact, disturbance has been shown to eliminate, rather than create, power-law structure in some systems (Kéfi et al. 2007).

Mussel bed recruitment facilitation in the field and laboratory

A species' spatial distribution may be due to what Halley et al. (2004) call "inheritance," where the pattern mirrors the distribution of necessary resources across the landscape. Perhaps mussels merely recruit to pieces of coarse sediment that have a power-law spatial distribution within a background of unsuitable mud and sand. Our field results were not consistent with this explanation. They supported our hypothesis (H_2) that mussels preferentially recruit to live mussel biogenic structure.

A spatial mismatch was discovered between the scales of variability in coarse sediment found in this study and in mussel abundance found by Commito et al. (2006) at the same time and locations. In addition, we found no significant positive correlations between mussels and any of the coarse sediment hard substrates. Mussels were not simply mapping onto a template of gravel and shell hash. However, recent larval recruits did have a significant positive correlation with one type of hard substrate: adult mussels. In addition, the field experiment showed that recruitment of all sizes of mussels was highest to live mussel substrate plots. Why did they not attach at equal rates to all of the three hard substrates? Live mussels may be the most advantageous substrate because they form a safe, stable matrix bound together by byssal threads (Dankers and Zuidema 1995, Dankers et al. 2001), whereas gravel and shell hash can tumble and slide across the bottom in bedload, damaging attached recruits. Live mussels also provide protection from predation within the byssal threads of large adults, increase fertilization success due to proximity of other reproductive individuals, and indicate suitable habitat requirements (Levitan 1991, McGrorty et al. 1993). Moreover, our attachment results demonstrated that almost all of the mussels at our sites were attached to other live mussels, by far the most common attachment. And of the many mussels attached to only one substrate category, the vast majority were attached to other live mussels. A likely scenario is that larval recruits and young mussels attach preferentially to other live mussels (Maas Geesteranus 1942, McGrorty et al. 1993) and remain attached as they become older and make more attachments to additional substrate categories.

The mechanisms behind recruitment facilitation remain unclear. Mussel chemical cues (de Vooys 2003) and byssal threads (McGrorty et al. 1990) are attractive to settlers and older recruits that engage in active crawling (Maas Geesteranus 1942, Uryu et al. 1996, Côté and Jelnikar 1999, de Vooys 2003, van de Koppel et al. 2005, 2008, Nicastro et al. 2007, Wang et al. 2009). The mussels in our laboratory experiment actively crawled, allowing them to encounter and attach to each other. This movement may have been directed by chemical cues as well as Lévy walks that led to the development of aggregations (de Jager et al. 2011). However, aggregation cannot be understood simply in terms of individual Lévy walk behavior. Mussels frequently moved as entire clumps rather than as individuals. Large mussels pushed and pulled clusters of other mussels, especially smaller ones.

Our field experiment was unique in that it specifically compared recruitment to live mussels and other forms of hard substrate on soft bottoms. Few of the recruits were recent larval settlers. Most were juveniles and adults that

actively crawled (including some carried along by crawling individuals) or were passively transported by water currents to existing mussel patches (Maas Geesteranus 1942, Bayne 1964, McGrorty et al. 1993, Reusch and Chapman 1995, 1997, Hunt and Scheibling 2001, Petrović and Guichard 2008, van de Koppel et al. 2008, Largaespada et al. 2012). The high rate of recruitment to live mussels that we observed indicates that transported mussels may have been more readily trapped by the vertical structure of live mussels than by other types of hard substrate. But vertical structure alone is not the entire story. Largaespada et al. (2012) demonstrated higher recruitment to live mussels than to empty mussel valves glued together and put in the same position as live mussels. Thus, recruitment of larvae and post-larvae to live mussels is likely to result from both passive transport and active crawling, followed by some combination of preferential attachment by the moving mussels and byssal thread trapping by the mussels toward which they move.

The laboratory experiment results supported the hypothesis (H_3) that juvenile and adult mussels self-organize into aggregations with power-law spatial structure. To our knowledge, these results are the first to document active mussel self-organization into power-law clusters. Aggregations in our laboratory experiment had more complex shapes than singletons, but they were also larger, resulting in significantly lower P:A ratios than for singletons. This P:A relationship helps explain why edge-related predation, thermal stress, and other threats decrease with aggregation size, while food limitation increases (Bertness and Grosholz 1985, Okamura 1986, Svane and Ompi 1993, Helmuth 1998, Commito and Dankers 2001, Casey and Chattopadhyay 2008, van de Koppel et al. 2008).

Soft-bottom mussel beds at most sites, including ours, seem to be regulated in ways that are different from those at the banded Wadden Sea and Menai Strait sites studied by Gascoigne et al. (2005) and van de Koppel et al. (2005, 2008). What might explain this difference? In the Wadden Sea, the band patterns are restricted to some so-called "young mussel beds" and are not the typical pattern observed there (Dankers et al. 2001, van de Koppel et al. 2005, 2012, Wang et al. 2009). At Menai Strait, bands occur at a site managed for mussel production by preparing the bottom and seeding manually with juvenile mussels (Gascoigne et al. 2005). In contrast, beds at our sites are not managed. They contain mussels of all ages and sizes (see size-class histograms from six sites in Commito et al. 2006). Water flow at our sites may cause sufficient turbulence along rough bottoms and irregular shorelines to eliminate food competition in laminar flow described at Wadden Sea and Menai Strait sites (Gascoigne et al. 2005, van de Koppel et al. 2005, 2008, Wang et al. 2009, Liu et al. 2012). At a Netherlands site similar to those in the Wadden Sea cited above, Capelle et al. (2014) established high- and low-density plots of uniformly distributed mussels on the sandy bottom. Within days the mussels began to aggregate into patchy arrays without bands. After three months the patchy distributions looked very similar to the spatial patterns observed at our sites in Maine and produced by our model and laboratory experiment. Thus, bands may be relatively rare phenomena occurring under special conditions not frequently met at most locations worldwide. Liu et al. (2012) call for caution in interpreting band spatial patterns and their emergent properties because the mechanisms regulating mussel bed spatial structure are poorly understood and require more empirical field and experimental analysis.

Implications

Soft-bottom mussel beds can exist in the same location for centuries (Obert and Michaelis 1991, Nehls and Thiel 1993, Herlyn and Millat 2000, Dolmer and Frandsen 2002, Büttger et al. 2014, Folmer et al. 2014). If mussels decline, patches of hard substrate remain in place and serve as future attachment sites, allowing beds to rebound. Our results indicate that live mussels are the most important type of hard substrate, more so than shell hash and gravel. From a resource management perspective, removal of mussel biogenic structure by dredging, raking, or other bed smoothing activities eliminates spatial memory. Disrupted recruitment facilitation is likely to change mussel abundance and spatial patterns, resulting in a cascade of subsequent effects that are not well understood (Dolmer and Frandsen 2002, Thrush et al. 2006, Gutiérrez et al. 2011). Better understanding of the onset, duration, and

management of these effects may result from research focused on the interaction between hard substrate availability and recruitment facilitation.

Acknowledgments

We thank B. Beal, A. Borowik, A. Commito, G. Commito, T. Crawford, P. Domenici, J. Fiorito, K. Fonte, S. Lilly, M. Mura, C. North, S. Olson, G. Protopropescu, R. Wilson, and the Downeast Institute for Applied Research and Education staff for their help, as well as the Dowling family for access to Bob's Cove. Comments from Martin Thiel and anonymous reviewers greatly improved the quality of this paper. This research was made possible by support for J. A. Commito from the Università di Pisa, a Gettysburg College Presidential Research Fellowship, and Gettysburg College Research and Professional Development grants; for N. J. Gownaris from a Garden Club of America summer research grant; and for W. E. Dow Piniak, B. M. Grupe, N. J. Gownaris, K. A. Reeves, and A. M. Vissichelli from Gettysburg College Senior Research Grants.

Literature Cited

Analytical Software. 2003. Statistix 8. Analytical Software, Tallahassee, Florida, USA.

Anselin, L. 2003. GeoDa 0.9 user's guide. Spatial Analysis Laboratory, University of Illinois, Urbana-Champaign, Illinois, USA.

Azovsky, A. I., M. V. Chertoprood, N. V. Kucheruk, P. V. Rybinov, and F. V. Sapozhnikov. 2000. Fractal properties of spatial distribution of intertidal benthic communities. Marine Biology 136:581–590.

Barabási, A.-L., and R. Albert. 1999. Emergence of scaling in random networks. Science 286:509–512.

Bayne, B. L. 1964. Primary and secondary settlement in *Mytilus edulis* L. (Mollusca). Journal of Animal Ecology 33:513–523.

Belt, K. M., S. W. B. Cole, and R. A. Scrosati. 2009. Intertidal barnacles as indicators of the intensity of scour by sea ice. Marine Ecology Progress Series 381:183–187.

Benedetti-Cecchi, L. 2001. Variability in abundance of algae and invertebrates at different spatial scales on rocky sea shores. Marine Ecology Progress Series 215:79–92.

Bertness, M. D., and E. Grosholz. 1985. Population dynamics of the ribbed mussel, *Geukensia demissa*: The costs and benefits of an aggregated distribution. Oecologia 67:192–204.

Bertness, M. D., G. C. Trussell, P. J. Ewanchuk, and B. R. Silliman. 2002. Do alternate stable community states exist in the Gulf of Maine rocky intertidal zone? Ecology 83:3434–3448.

Bishop, M. J., A. J. Underwood, and P. Archambault. 2002. Sewage and environmental impacts on rocky shores: necessity of identifying relevant spatial scales. Marine Ecology Progress Series 236:121–128.

Bouma, T. J., S. Olenin, K. Reise, and T. Ysebaert. 2009. Ecosystem engineering and biodiversity in coastal sediments: posing hypotheses. Helgoland Marine Research 63:95–106.

Brinkman, A., N. Dankers, and M. van Stralen. 2002. An analysis of mussel bed habitats in the Dutch Wadden Sea. Helgoland Marine Research 56:59–75.

Büttger, H., G. Nehls, and P. Stoddard. 2014. The history of intertidal blue mussel beds in the North Frisian Wadden Sea in the 20th century: can we define conditions for conservation targets by analyzing aerial photographs? Journal of Sea Research 87:91–102.

Capelle, J. J., J. W. M. Wijsman, T. Schellekens, M. R. van Stralen, P. M. J. Herman, and A. C. Small. 2014. Spatial organization and biomass development after relaying of mussel seed. Journal of Sea Research 85:395–403.

Casey, M. M., and D. Chattopadhyay. 2008. Clumping behavior as a strategy against drilling predation: Implications for the fossil record. Journal of Marine Biology and Ecology 367:174–179.

Commito, J. A. 1987. Adult-larval interactions: predictions, mussels, and cocoons. Estuarine, Coastal and Shelf Science 25:599–606.

Commito, J. A., E. A. Celano, H. J. Celico, S. Como, and C. P. Johnson. 2005. Mussels matter: postlarval dispersal dynamics altered by a spatially complex ecosystem engineer. Journal of Experimental Marine Biology and Ecology 316:133–147.

Commito, J. A., S. Como, B. M. Grupe, and W. E. Dow. 2008. Species diversity in the soft-bottom intertidal zone: biogenic structure, sediment, and macrofauna across mussel bed spatial scales. Journal of Experimental Marine Biology and Ecology 366:70–81.

Commito, J. A., and N. Dankers. 2001. Dynamics of spatial and temporal complexity in European and North American soft-bottom mussel beds. Pages 39–59 *in* K. Reise, editor. Ecological comparisons of sedimentary shores. Springer-Verlag, Heidelberg, Germany.

Commito, J. A., W. E. Dow, and B. M. Grupe. 2006. Hierarchical spatial structure in soft-bottom mussel beds. Journal of Experimental Marine Biology and Ecology 330:27–37.

Commito, J. A., and B. R. Rusignuolo. 2000. Structural complexity in mussel beds: the fractal geometry of surface topography. Journal of Experimental Marine Biology and Ecology 225:133–152.

Commito, J. A., and G. Tita. 2002. Differential dispersal rates in an intertidal meoifauna assemblage. Journal of Experimental Marine Biology and

Ecology 268:237–256.
Côté, I. M., and E. Jelnikar. 1999. Predator-induced clumping behavior in mussels (*Mytilus edulis* Linnaeus). Journal of Experimental Marine Biology and Ecology 235:201–211.
Crawford, T. W., J. A. Commito, and A. M. Borowik. 2006. Fractal characterization of *Mytilus edulis* L. spatial structure in intertidal landscapes using GIS methods. Landscape Ecology 21:1033–1044.
Dankers, N., A. G. Brinkman, A. Meijboom, and E. Dijkman. 2001. Recovery of intertidal mussel beds in the Waddensea: use of habitat maps in the management of the fishery. Hydrobiologia 465:21–30.
Dankers, N., and D. R. Zuidema. 1995. The role of the mussel (*Mytilus edulis* L.) and mussel culture in the Dutch Wadden Sea. Estuaries 18:71–80.
de Jager, M., F. J. Weissing, P. M. J. Herman, B. A. Nolet, and J. van de Koppel. 2011. Lévy walks evolve through interaction between movement and environmental complexity. Science 332:1551–1553.
de Vooys, C. G. N. 2003. Effect of a tripeptide on the aggregational behavior of the blue mussel *Mytilus edulis*. Marine Biology 142:1119–1123.
Dolmer, P., and R. P. Frandsen. 2002. Evaluation of the Danish mussel fishery: suggestions for an ecosystem approach. Helgoland Marine Research 56:13–20.
Donadi, S., T. van der Heide, E. M. van der Zee, J. S. Eklöf, J. van de Koppel, E. J. Weerman, T. Piersma, H. Olff, and B. K. Eriksson. 2013. Cross-habitat interactions among bivalve species control community structure on intertidal flats. Ecology 94:489–498.
Dungan, J. L., J. N. Perry, M. R. T. Dale, P. Legendre, S. Citron-Pousty, M.-J. Fortin, A. Jakomulska, M. Miriti, and M. S. Rosenberg. 2002. A balanced view of scale in spatial statistical analysis. Ecography 25:626–640.
Environmental Systems Research Institute. 2006. ESRI, Redlands, California, USA.
Fletcher, D. J., and A. J. Underwood. 2002. How to cope with negative estimates of components of variance in ecological field studies. Journal of Experimental Marine Biology and Ecology 273:89–95.
Folmer, E. O., J. Drent, K. Troost, H. Büttger, N. Dankers, J. Jansen, M. van Stralen, G. Millat, M. Herlyn, and C. J. Philippart. 2014. Large-scale spatial dynamics of intertidal mussel (*Mytilus edulis* L.) bed coverage in the German and Dutch Wadden Sea. Ecosystems 17:550–566.
Gascoigne, J. C., H. A. Beadman, C. Saurel, and M. J. Kaiser. 2005. Density dependence, spatial scale and patterning in sessile biota. Oecologia 145:371–381.
Guichard, F., P. M. Halpin, G. W. Allison, J. Lubchenco, and B. A. Menge. 2003. Mussel disturbance dynamics: signatures of oceanographic forcing from local interactions. American Naturalist 161:889–904.
Guillemette, M., and J. H. Himmelman. 1996. Distribution of wintering common eiders over mussel beds: does the ideal free distribution apply? Oikos 76:435–442.
Gutiérrez, J. L., C. G. Jones, J. E. Byers, K. K. Arkema, K. Berkenbusch, J. A. Commito, C. M. Duarte, S. D. Hacker, J. G. Lambrinos, I. E. Hendriks, P. J. Hogarth, M. G. Palomo, and C. Wild. 2011. Physical ecosystem engineers and the functioning of estuaries and coasts. Pages 53–81 *in* E. Wolanski E. and D. S. McLusky, editors. Treatise on estuarine and coastal science, Vol 7: Functioning of ecosystems at the land-ocean interface. Elsevier, Academic Press, Waltham, Massachusetts, USA.
Haining, R. 1990. Spatial data analysis in the social and environmental sciences. Cambridge University Press, Cambridge, UK.
Halley, J. M., S. Hartley, A. S. Kallimanis, W. E. Kunin, and S. P. Sgardelis. 2004. Uses and abuses of fractal methodology in ecology. Ecology Letters 7:254–271.
Hamilton, D. J. 2000. Direct and indirect effects of predation by common eiders and abiotic disturbance in an intertidal community. Ecological Monographs 70:21–43.
Hamilton, D. J., T. D. Nudds, and J. Neate. 1999. Size-selective predation of blue mussels (*Mytilus edulis*) by common eiders (*Somateria mollissima*) under controlled field conditions. The Auk 116:403–416.
Hastings, H. M., and G. Sugihara. 1993. Fractals: A user's guide for the natural sciences. Oxford University Press, Oxford, UK.
Hayhurst, S., and P. D. Rawson. 2009. Species-specific variation in larval survival and patterns of distribution for the blue mussels *Mytilus edulis* and *Mytilus trossulus* in the Gulf of Maine. Journal of Molluscan Studies 75:215–222.
Helmuth, B. S. T. 1998. Intertidal mussel microclimates: predicting the body temperature of a sessile invertebrate. Ecological Monographs 68:51–74.
Herlyn, M., and G. Millat. 2000. Decline of the intertidal blue mussel (*Mytilus edulis*) stock at the coast of Lower Saxony (Wadden Sea) and influence of mussel fishery on the development of young mussel beds. Hydrobiologia 426:203–210.
Herlyn, M., G. Millat, and B. Petersen. 2008. Documentation of sites of intertidal blue mussel (*Mytilus edulis* L.) beds of the Lower Saxonian Wadden Sea, southern North Sea (as of 2003) and the role of their structure for spatfall settlement. Helgoland Marine Research 62:177–188.
Hunt, H. L., and R. E. Scheibling. 2001. Patch dynamics of mussels on rocky shores: integrating process to understand pattern. Ecology 82:3213–3231.

Kéfi, S., M. Reitkerk, C. L. Alados, Y. Pueyo, V. P. Papanastasis, A. ElAich, and P. C. de Ruiter. 2007. Spatial vegetation patterns and imminent desertification in Mediterranean arid ecosystems. Nature 449:213–217.

Kostylev, V., and J. Erlandsson. 2001. A fractal approach for detecting spatial hierarchy and structure on mussel beds. Marine Biology 139:497–506.

Largaespada, C., F. Guichard, and P. Archambault. 2012. Meta-ecosystem engineering: Nutrient fluxes reveal intraspecific and interspecific feedbacks in fragmented mussel beds. Ecology 93:324–333.

Levin, S. A. 1999. Fragile dominion: complexity and the commons. Helix Books, Reading Massachusetts, USA.

Levitan, D. R. 1991. Influence of body size and population density on fertilization success and reproductive output in a free-spawning invertebrate. Biological Bulletin 181:261–268.

Liu, Q.-X., E. J. Weerman, P. M. J. Herman, H. Olff, and J. van de Koppel. 2012. Alternative mechanisms alter the emergent properties of self-organization in mussel beds. Proceedings of the Royal Society B: Biological Sciences 279:2744–2753.

Maas Geesteranus, R. A. 1942. On the formation of banks by *Mytilus edulis* L. Archives Néerlandaises Zoologie 6:283–326.

McArdle, B. H., J. E. Hewitt, and S. F. Thrush. 1997. Pattern from process: it is not as easy as it looks. Journal of Experimental Marine Biology and Ecology 216:229–242.

McGrorty, S., R. T. Clarke, C. J. Reading, and J. D. Goss-Custard. 1990. Population dynamics of the mussel *Mytilus edulis*: density changes and regulation of the population in the Exe estuary, Devon. Marine Ecology Progress Series 67:157–169.

McGrorty, S., J. D. Goss-Custard, and R. T. Clarke. 1993. Mussel *Mytilus edulis* (Mytiliacea) dynamics in relation to environmental gradients and intraspecific interactions. Netherlands Journal of Aquatic Ecology 27:163–171.

Nehls, G., and M. Thiel. 1993. Large-scale distribution patterns of the mussel *Mytilus edulis* in the Wadden Sea of Schleswig–Holstein: do storms structure the ecosystem? Netherlands Journal of Sea Research 31:181–187.

Nicastro, K. R., G. I. Zardi, and C. D. McQuaid. 2007. Behavioural response of invasive *Mytilus galloprovincialis* and indigenous *Perna perna* mussels exposed to risk of predation. Marine Ecology Progress Series 336:169–175.

Obert, B., and H. Michaelis. 1991. History and ecology of the mussel beds (*Mytilus edulis* L.) in the catchment area of a Wadden Sea tidal inlet. Pages 185–194 *in* M. Elliot and J.-P. Ducrotoy, editors. Estuaries and coasts: spatial and temporal intercomparisons. Olsen and Olsen, Viborg, Denmark.

Okamura, B. 1986. Group living and the effects of spatial position in aggregations of *Mytilus edulis*. Oecologia 69:341–347.

Pascual, M., and F. Guichard. 2005. Criticality and disturbance in spatial ecological systems. Trends in Ecology and Evolution 20:88–95.

Petrović, F., and F. Guichard. 2008. Scales of *Mytilus* spp. population dynamics: importance of adult displacement and aggregation. Marine Ecology Progress Series 356:203–214.

Reusch, T. B. H., and A. R. O. Chapman. 1995. Storm effects on eelgrass (*Zostera marina* L.) and blue mussel (*Mytilus edulis* L.) beds. Journal of Experimental Marine Biology and Ecology 192:257–271.

Reusch, T. B. H., and A. R. O. Chapman. 1997. Persistence and space occupancy by subtidal blue mussel patches. Ecological Monographs 67:65–87.

Riginos, C., and C. W. Cunningham. 2005. Local adaptation and species segregation in two mussel (*Mytilus edulis* × *Mytilus trossulus*) hybrid zones. Molecular Ecology 14:381–400.

Scanlon, T. M., K. C. Caylor, S. A. Levin, and I. Rodriguez-Iturbe. 2007. Positive feedbacks promote power-law clustering of Kalahari vegetation. Nature 449:209–212.

Snover, M. L., and J. A. Commito. 1998. The fractal geometry of *Mytilus edulis* L. spatial distribution in a soft-bottom system. Journal of Experimental Marine Biology and Ecology 223:53–64.

Sokal, R. R., and F. J. Rohlf. 1995. Biometry. W. H. Freeman, New York, New York, USA.

SPSS. 2006. SPSS for Windows, Rel. 15. SPSS, Chicago, Illinois, USA.

Stillman, R. A., S. McGrorty, J. D. Goss-Custard, and A. D. West. 2000. Predicting mussel population density and age structure: the relationship between model complexity and predictive power. Marine Ecology Progress Series 208:131–145.

Svane, I., and M. Ompi. 1993. Patch dynamics in beds of the blue mussel *Mytilus edulis* L.: effects of site, patch size, and position within a patch. Ophelia 37:187–192.

Tam, J. C., and R. A. Scrosati. 2014. Distribution of cryptic mussel species (*Mytilus edulis* and *M. trossulus*) along wave exposure gradients on northwest Atlantic rocky shores. Marine Biology Research 10:51–60.

Thrush, S. F., J. S. Gray, J. E. Hewitt, and K. I. Ugland. 2006. Predicting the effects of habitat homogenization on marine biodiversity. Ecological Applications 16:1636–1642.

TruSoft. 2004. Benoit 1.3 Fractal Analysis System. TruSoft International, St. Petersburg, Florida, USA.

Underwood, A. J. 1997. Experiments in ecology: their logical design and interpretation using analysis of variance. Cambridge University Press, Cambridge,

UK.
Uryu, Y., K. Iwasaki, and M. Hinoue. 1996. Laboratory experiments on behaviour and movement of a freshwater mussel, *Limnoperna fortunei* (Dunker). Journal of Molluscan Studies 62:327–341.
van de Koppel, J., T. J. Bouma, and P. M. J. Herman. 2012. The influence of local-and landscape-scale processes on spatial self-organization in estuarine ecosystems. 2012. Journal of Experimental Biology 215:962–967.
van de Koppel, J., J. C. Gascoigne, G. Theraulaz, M. Rietkerk, W. M. Mooij, and P. M. J. Herman. 2008. Experimental evidence for spatial self-organization and its emergent effects in mussel bed ecosystems. Science 322:739–742.
van de Koppel, J., M. Rietkerk, N. Dankers, and P. M. J. Herman. 2005. Scale-dependent feedback and regular spatial patterns in young mussel beds. American Naturalist 165:E66–E77.
Visual Basic 6.0. 1999. Microsoft Corporation, Redmond, Washington, USA.
wa Kangeri, A. K., J. M. Jansen, B. R. Barkman, J. J. A. Donker, D. J. Joppe, and N. M. J. A. Dankers. 2014. Perturbation induced changes in substrate use by the blue mussel, *Mytilus edulis*, in sedimentary systems. Journal of Sea Research 85:233–240.
Wang, R.-H., Q.-X. Liu, G.-Q. Sun, Z. Jin, and J. van de Koppel. 2009. Nonlinear dynamic and pattern bifurcations in a model for spatial patterns in young mussel beds. Journal of the Royal Society Interface 6:705–718.
Wootton, J. T. 2001. Local interactions predict large-scale pattern in empirically derived cellular automata. Nature 413:841–844.
Zar, J. H. 1999. Biostatistical analysis. Fourth edition. Prentice Hall, Upper Saddle River, New Jersey, USA.

Supplemental Material

Appendix A

Recruitment Facilitation Model Description

The Recruitment Facilitation Model (see Supplement for source code and executable file with interface for readers to use) allows the user to choose from four distinctly paired rules called "Edge" (recruitment facilitation at patch edge), ''No Edge'' (recruitment at any location), "Growth" (recruitment with bed growth), and "No Growth" (recruitment without bed growth), creating four possible scenarios (Scenarios 1–4, below). If desired, each of the four rules may be applied to a mussel bed where the user can spatially structure the probability of recruitment success, creating four additional scenarios (Scenarios 5–8, below).

Note that Scenario 1 was utilized in this paper.

The executable file opens to an interface that allows the user to choose the desired scenario ("Rule" box), number of initial recruitment sites, number of iterations, and number of filled cells (the latter for the No Growth scenarios, i.e., Scenarios 3, 4, 7, 8). For the spatially structured scenarios (Scenarios 5–8), the user chooses the probability values and area values for colored blocks (R = red, O = orange, etc.) located randomly within the lattice.

Scenario 1: Recruitment facilitation, with mussel bed growth: "Edge" and "Growth" rules applied.— The bed is represented by a square lattice C of 100×100 cells having at most four orthogonal neighbors (von Neumann neighborhood). The borders are not wraparound. Each cell may obtain one of two values, 0 (empty) or 1 (filled), representing absence or presence of mussels, respectively. After an initial random selection of filled initial recruitment sites, the lattice is updated asynchronously according to two rules: *Edge = recruitment may occur only within the von Neumann neighborhood of a filled cell (i.e., at a patch edge),* and *Growth = patches are allowed to grow (i.e., mussels are not removed from filled cells).* This scenario represents the attachment of recruits at the edges of mussel patches, including the edges of interior gaps, causing an increase in bed cover.

Let $C^t_{i,j}$ represent the value of the cell at lattice position (i, j) for discrete time step t, where $t = 0$,

1, 2, 3. . . , n.

a. At the initial time step $t = 0$, the lattice contains any number of randomly assigned filled initial recruitment sites whose values are set to 1. All remaining cells have value 0.
b. For each subsequent time step t, one ordered pair of independent random positive integers (i, j) between 1 and 100 inclusive is generated.

Apply the following transition rule:

$$\text{If } C_{i,j}^{t} = 0 \text{ and } C_{i,j-1}^{t} + C_{i,j+1}^{t} + C_{i-1,j}^{t} + C_{i+1,j}^{t} > 0$$

$$\text{Then } C_{i,j}^{t+1} = 1$$

$$\text{Else } C_{i,j}^{t+1} = C_{i,j}^{t}$$

c. The updating process may be terminated in one of two pre-determined ways: At a given time step, $t = n$, or when a given number of filled cells, $0 \leq m \leq 10000$, have been added to the lattice.

Scenario 2: No recruitment facilitation, but with bed growth: "No Edge" and "Growth" rules applied.—The bed is represented by a lattice of 100 × 100 square cells. The borders are not wraparound. Each cell may obtain one of two values, 0 (empty) or 1 (filled), representing absence or presence of mussels, respectively. After an initial random selection of filled initial recruitment sites, the lattice is updated asynchronously according to two rules: *No Edge = recruitment may occur anywhere within the lattice,* and *Growth = patches are allowed to grow (i.e., mussels are not removed from filled cells)*. This scenario represents random accumulation of recruits anywhere on bare sediment, including, but not limited to, the edges of patches and interior gaps.

Let $C_{i,j}^{t}$ represent the value of the cell at lattice position (i, j) for discrete time step t, where $t = 0$, 1, 2, 3. . . , n.

a. At the initial time step $t = 0$, the lattice contains any number of randomly assigned filled initial recruitment sites whose values are set to 1. All remaining cells have value 0.
b. For each subsequent time step t, one ordered pair of independent random positive integers (i, j) between 1 and 100 inclusive is generated.

Apply the following transition rule:

$$\text{If } C_{i,j}^{t} = 0$$

$$\text{Then } C_{i,j}^{t+1} = 1$$

$$\text{Else } C_{i,j}^{t+1} = C_{i,j}^{t}$$

c. The updating process may be terminated in one of two pre-determined ways: At a given time step, $t = n$, or when a given number of filled cells, $0 \leq m \leq 10000$, have been added to the lattice.

Scenario 3: Recruitment facilitation, no bed growth: "Edge" and "No Growth" rules applied.—The bed is represented by a square lattice of 100 × 100 cells, with each cell having at most four orthogonal neighbors (von Neumann neighborhood). The borders are not wraparound. Cells are either in the empty state or the filled state, representing absence or presence of mussels, respectively. After populating the bed with an initial random selection of filled cells, the lattice is updated asynchronously according to two rules: *Edge = recruitment may occur only within the von Neumann neighborhood of a filled cell (i.e., at a patch edge),* and *No Growth = for every cell that becomes filled with a recruit, a mussel is removed from another already filled cell*. This scenario represents no net change in bed cover, with recruitment at the edges of mussel patches, including the edges of interior gaps, and removal occurring anywhere in the system.

Let $C_{i,j}^{t}$ represent the value of the cell at lattice position (i, j) for discrete time step t, where $t = 0$, 1, 2, 3. . . , n.

a. At the initial time step $t = 0$, the lattice contains any number of randomly assigned filled cells whose values are set to 1. All remaining cells have value 0.
b. For each subsequent time step t, two ordered pairs of independent random positive integers ($m1$, $n1$) and ($m2$, $n2$) between 1 and 100 inclusive, for which $C_{m1,n1}^{t} = 0$and $C_{m2,n2}^{t} = 1$, are generated.

Apply the following transition rule:

$$\text{If } (i,\ j)\ =\ (m1,\ n1) \text{ and } C^t_{i,j-1} + C^t_{i,j+1} + C^t_{i-1,j} + C^t_{i+1,j} > 0$$

$$\text{Then } C^{t+1}_{i,j} = 1 \text{ and } C^{t+1}_{m1,n2} = 0$$

$$\text{Else } C^{t+1}_{i,j} = C^t_{i,j}$$

c. The updating process may be terminated in one pre-determined way: At a given time step, $t = n$.

Scenario 4: No recruitment facilitation, no bed growth: "No Edge" and "No Growth" rules applied.—The bed is represented by a square lattice of 100×100 cells, with each cell having at most four orthogonal neighbors (von Neumann neighborhood). The borders are not wraparound. Cells are either in the empty state or the filled state, representing absence or presence of mussels, respectively. After populating the bed with an initial random selection of filled cells, the lattice is updated asynchronously according to two rules: *No Edge = recruitment may occur anywhere within the lattice,* and *No Growth = for every cell that becomes filled with a recruit, a mussel is removed from another already filled cell*. This scenario represents no net change in bed cover, with recruitment and removal occurring anywhere in the system.

Let $C^t_{i,j}$ represent the value of the cell at lattice position (i, j) for discrete time step t, where $t = 0, 1, 2, 3\ldots, n$.

a. At the initial time step $t = 0$, the lattice contains any number of randomly assigned filled cells whose values are set to 1. All remaining cells have value 0.
b. For subsequent time steps two ordered pairs of independent random positive integers $(m1, n1)$ and $(m2, n2)$ between 1 and 100 inclusive, for which $C^t_{m1,n1} = 0$and $C^t_{m2,n2} = 1$ are generated.

Apply the following transition rule:

$$\text{If } (i,\ j)\ =\ (m1,\ n1)$$

$$\text{Then } C^{t+1}_{i,j} = 1 \text{ and } C^{t+1}_{m2,n2} = 0$$

$$\text{Else } C^{t+1}_{i,j} = C^t_{i,j}$$

c. The updating process may be terminated in one pre-determined way: At a certain time step, $t = n$.

Scenario 5: Recruitment facilitation, with mussel bed growth: "Edge" and "Growth" rules applied to mussel bed where the user spatially structures the probability of recruitment success.—Identical to Scenario 1 (above), except that recruitment may occur with some degree of probability only within the von Neumann neighborhood of a filled cell (i.e., at an edge).

Let $C^t_{i,j}$ represent the value of the cell at lattice C position (i, j) for discrete time step t, where $t = 0, 1, 2, 3\ldots, n$.

Let P be a related square lattice of 100×100 cells, such that cell $C^t_{i,j}$ has recruitment probability $P_{i,j}$. In lattice P, the 100×100 cells are subdivided into 10-square blocks, such that cells within the same block possess the same recruitment probability.

a. At the initial time step $t = 0$, lattice C contains any number of randomly assigned filled initial recruitment sites whose values are set to 1. All remaining cells have value 0. In addition, the 100 10-square blocks of probability lattice P are filled according to a pre-determined set of probabilities and related areas (blocks) containing those probabilities.
b. For each subsequent time step t, three independent random numbers are generated: one ordered pair of random positive integers (i, j) between 1 and 100 inclusive, and one random real number $0 \leq r < 1$.

Apply the following transition rule:

$$\text{If } C^t_{i,j} = 0 \text{ and } C^t_{i,j-1} + C^t_{i,j+1} + C^t_{i-1,j} + C^t_{i+1,j} > 0 \text{ and } r < P_{i,j}$$

$$\text{Then } C^{t+1}_{i,j} = 1$$

$$\text{Else } C^{t+1}_{i,j} = C^t_{i,j}$$

c. The updating process may be terminated in one of two pre-determined ways: At a given time step, $t = n$, or when a given number of filled cells, $0 \leq m \leq 10000$ have been added to the lattice.

Scenario 6: No recruitment facilitation, but with bed growth: "No Edge" and "Growth" rules applied

to mussel bed where the user spatially structures the probability of recruitment success.—Identical to Scenario 2 (above), except that recruitment may occur with some degree of probability anywhere within the lattice.

Let $C^t_{i,j}$represent the value of the cell at lattice C position (i, j) for discrete time step t, where $t = 0$, 1, 2, 3. . . , n.

Let P be a related square lattice of 100 × 100 cells, such that cell $C_{i,j}$ has recruitment probability$P_{i,j}$. In lattice P, the 100 × 100 cells are subdivided into 10-square blocks, such that cells within the same block possess the same recruitment probability.

a. At the initial time step $t = 0$, lattice C contains any number of randomly assigned filled initial recruitment sites whose values are set to 1. All remaining cells have value 0. In addition, the 100 10-square blocks of probability lattice P are filled according to a pre-determined set of probabilities and related areas (blocks) containing those probabilities.
b. For each subsequent time step t, three independent random numbers are generated: one ordered pair of random positive integers (i, j) between 1 and 100 inclusive, and one random real number $0 \leq r < 1$.

Apply the following transition rule:

$$\text{If } C^t_{i,j} = 0 \text{ and } r < P_{i,j}$$

$$\text{Then } C^{t+1}_{i,j} = 1$$

$$\text{Else } C^{t+1}_{i,j} = C^t_{i,j}$$

c. The updating process may be terminated in one of two pre-determined ways: At a given time step, $t = n$, or when a given number of filled cells, $0 \leq m \leq 10000$ have been added to the lattice.

Scenario 7: Recruitment facilitation, no bed growth: "Edge" and "No Growth" rules applied to mussel bed where the user spatially structures the probability of recruitment success.—Identical to Scenario 3 (above), except that recruitment may occur with some degree of probability only within the von Neumann neighborhood of a filled cell (i.e., at an edge).

Let $C^t_{i,j}$ represent the value of the cell at lattice position (i, j) for discrete time step t, where $t = 0$, 1, 2, 3. . . , n.

Let P be a related square lattice of 100 × 100 cells, such that cell $C_{i,j}$has recruitment probability $P_{i,j}$. In lattice P, the 100 × 100 cells are subdivided into 10-square blocks, such that cells within the same block possess the same recruitment probability.

a. At the initial time step $t = 0$, lattice C contains any number of randomly assigned filled cells whose values are set to 1. All remaining cells have value 0. In addition, the 100 10-square blocks of probability lattice P are filled according to a predetermined set of probabilities and related areas (blocks) containing those probabilities.
b. For each subsequent time step t, two ordered pairs of independent random positive integers ($m1$, $n1$) and ($m2$, $n2$) between 1 and 100 inclusive , for which $C^t_{m1,n1} = 0$and $C^t_{m2,n2} = 1$, and one random real number $0 \leq r < 1$ are generated.

Apply the following transition rule:

$$\text{If } (i,\ j) = (m1,\ n1) \text{ and } C^t_{i,j-1} + C^t_{i,j+1} + C^t_{i-1,j} + C^t_{i+1,j} > 0 \text{ and } r < P_{i,j}$$

$$\text{Then } C^{t+1}_{i,j} = 1 \text{ and } C^{t+1}_{m2,n2} = 0$$

$$\text{Else } C^{t+1}_{i,j} = C^t_{i,j}$$

c. The updating process may be terminated in one pre-determined way: At a given time step, $t = n$.

Scenario 8: No recruitment facilitation, no bed growth: "No Edge" and "No Growth" rules applied to mussel bed where the user spatially structures the probability of recruitment success.—Identical to Scenario 4 (above), except that recruitment may occur with some degree of probability anywhere within the lattice.

Let $C^t_{i,j}$ represent the value of the cell at lattice position (i, j) for discrete time step t, where $t = 0$, 1, 2, 3. . . , n.

Let P be a related square lattice of 100 × 100 cells, such that cell $C_{i,j}$ has recruitment probability $P_{i,j}$. In lattice P, the 100 × 100 cells are subdivided into 10-square blocks, such that cells within the same block possess the same recruit-

ment probability.

a. At the initial time step $t = 0$, the lattice contains any number of randomly assigned filled cells whose values are set to 1. All remaining cells have value 0.
b. For subsequent time steps two ordered pairs of independent random positive integers ($m1$, $n1$) and ($m2$, $n2$) between 1 and 100 inclusive, for which $C^t_{m1,n1} = 0$ and $C^t_{m2,n2} = 1$, and one random real number $0 \leq r < 1$ are generated.

Apply the following transition rule:

$$\text{If } (i,\ j) = (m1,\ n1) \text{ and } r < P_{i,j}$$

$$\text{If } C^{t+1}_{i,j} = 1 \text{ and } C^{t+1}_{m2,n2} = 0$$

$$\text{Else } C^{t+1}_{i,j} = C^t_{i,j}$$

c. The updating process may be terminated in one pre-determined way: At a given time step, $t = n$.

APPENDIX B

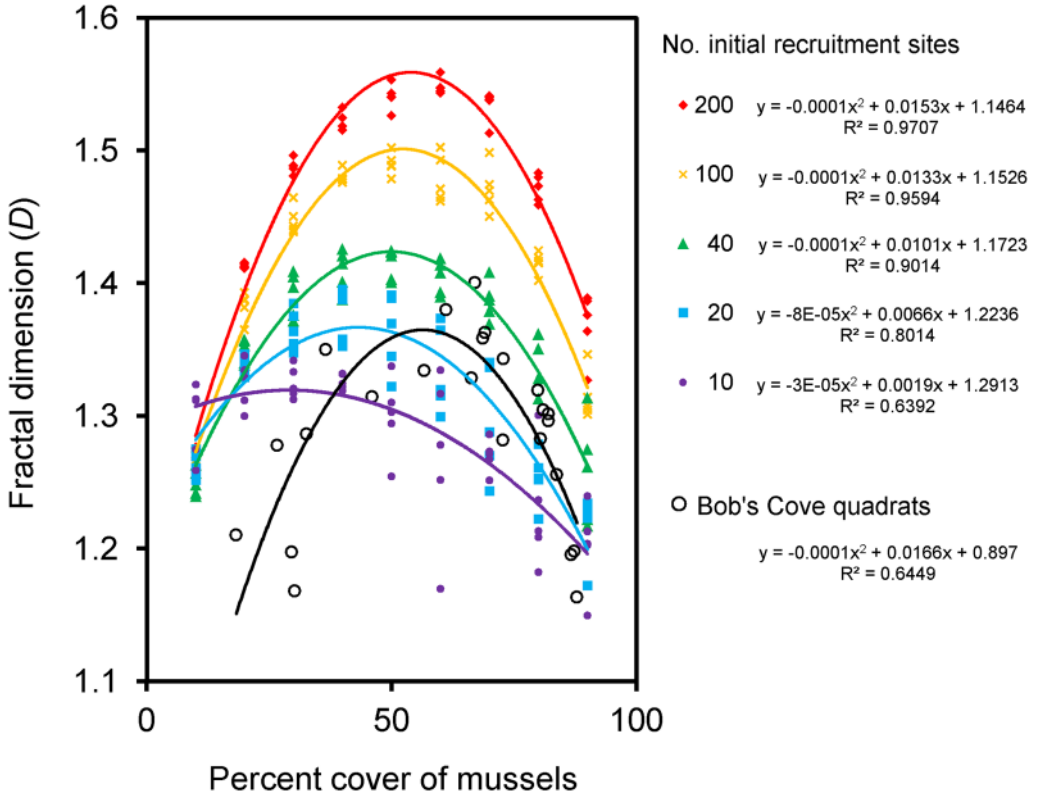

Fig. B1. Expanded version of Fig. 7, with data points and regression equations. See Fig. 7 legend for details.

Appendix C

ANOVA and Tukey HSD all-pairwise comparison tables for recruitment experiment

Table C1. Analysis of variance table for recruitment experiment.

Source	df	SS	MS	*F*	*P*
Block (A)	9	55.60	6.178	0.52	0.382
Site (B)	2	21.79	10.893	0.92	0.4147
Error A × B	18	212.08	11.782		
Substrate (C)	4	651.50	162.875	26.77	**0.0000**
B × C	8	99.68	12.460	2.05	**0.0473**
Error A × B × C	108	657.02	6.084		
Habitat (D)	1	324.48	324.480	37.67	**0.0000**
B × D	2	40.56	20.280	2.35	0.1141
Error A × B × D	27	232.56	8.613		
C × D	4	316.55	79.138	18.73	**0.0000**
B × C × D	8	32.51	4.063	0.96	0.4699
Error A × B × C × D	108	456.34	4.225		
Total	299	3100.6			

Note: Significant differences appear in boldface.

Table C2. Tukey HSD all-pairwise comparisons tests for recruitment experiment.

Factor	Mean	Homogeneous groups
Site		
Carrying Place Cove	2.400	A
Guard Point	2.060	A
Hammond Cove	1.740	A
Substrate		
Live mussels	4.417	A
Ambient cores	3.10	B
Mussel shell hash	1.40	C
Gravel	0.967	C
Muddy sand	0.450	C
Habitat		
Mussel	3.107	A
Bare sediment	1.027	B

Note: Alpha = 0.05.

Supplement

Recruitment facilitation model source code and executable file with interface (*Ecological Archives* http://dx.doi.org/10.1890/ES14-00200.1.sm).